Supplementary Information for Journal of Vertebrate Paleontology

Simbakubwa kutokaafrika (Hyaenodonta, "Creodonta", Mammalia) from the earliest Miocene of Kenya and the evolution of gigantic hyaenodonts

MATTHEW R. BORTHS[1*] and NANCY J. STEVENS[2]

[1] Department of Biomedical Sciences, Heritage College of Osteopathic Medicine, Ohio Center for Ecology and Evolutionary Studies, Ohio University, Athens OH, 45701 U.S.A., matthew.borths@duke.edu;
[2] Department of Biomedical Sciences, Heritage College of Osteopathic Medicine, Ohio Center for Ecology and Evolutionary Studies, Ohio University, Athens OH, 45701 U.S.A., stevensn@ohio.edu

[*] Corresponding author

Table of Contents

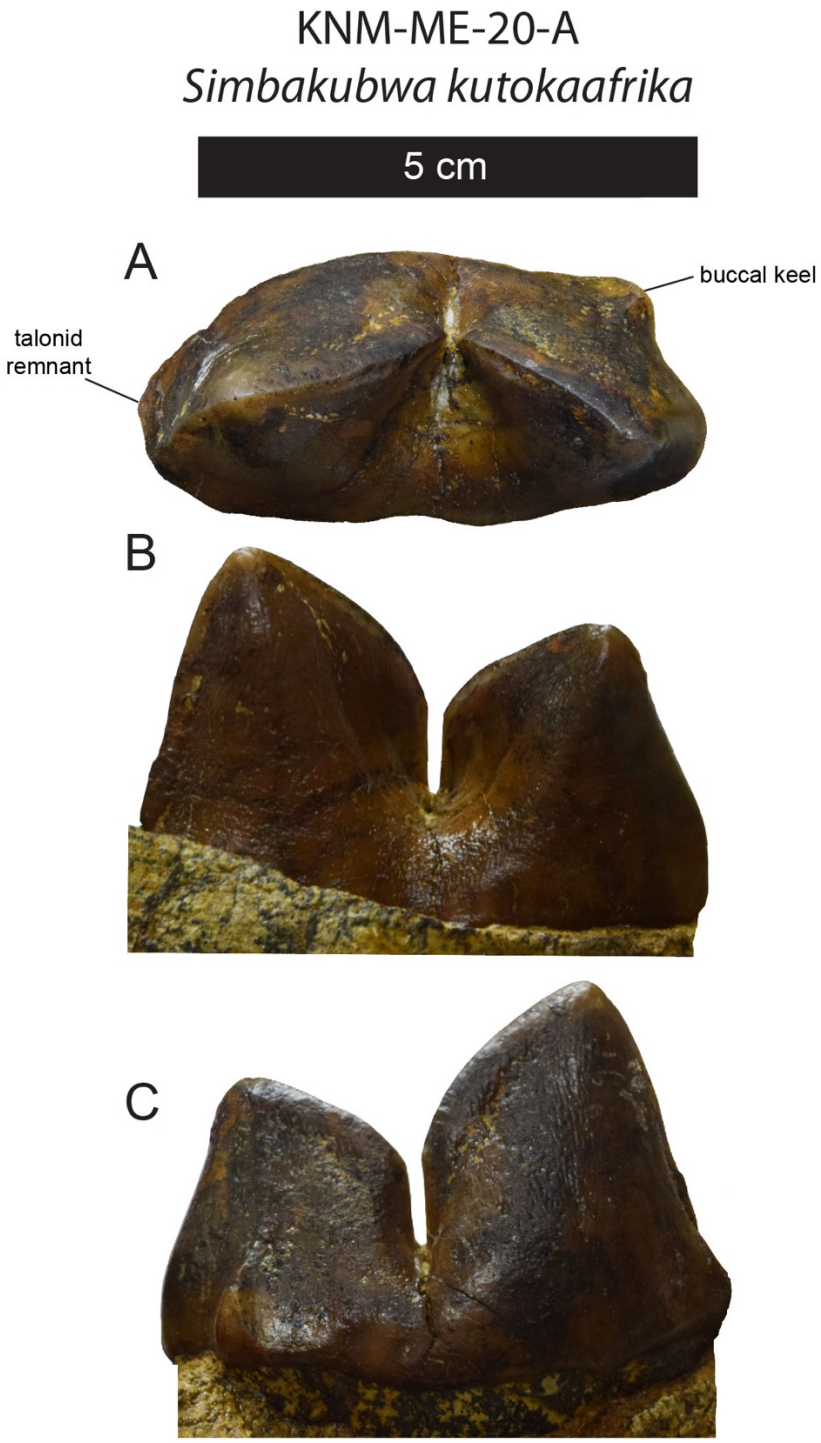

FIGURE 1S. Additional views of *Simbakubwa* holotype left m3 (KNM-ME 20A). **A**, Occlusal view; **B**, lingual view; **C**, buccal view. Note the robust buccal keel on the protoconid that would have braced the talonid of m2 and the very reduced talonid remnant on the distal aspect of the paraconid. 3D rendering of the specimen is also accessible as part of Project 483 at <www.morphosource.org>. Scale bar is 5 cm.

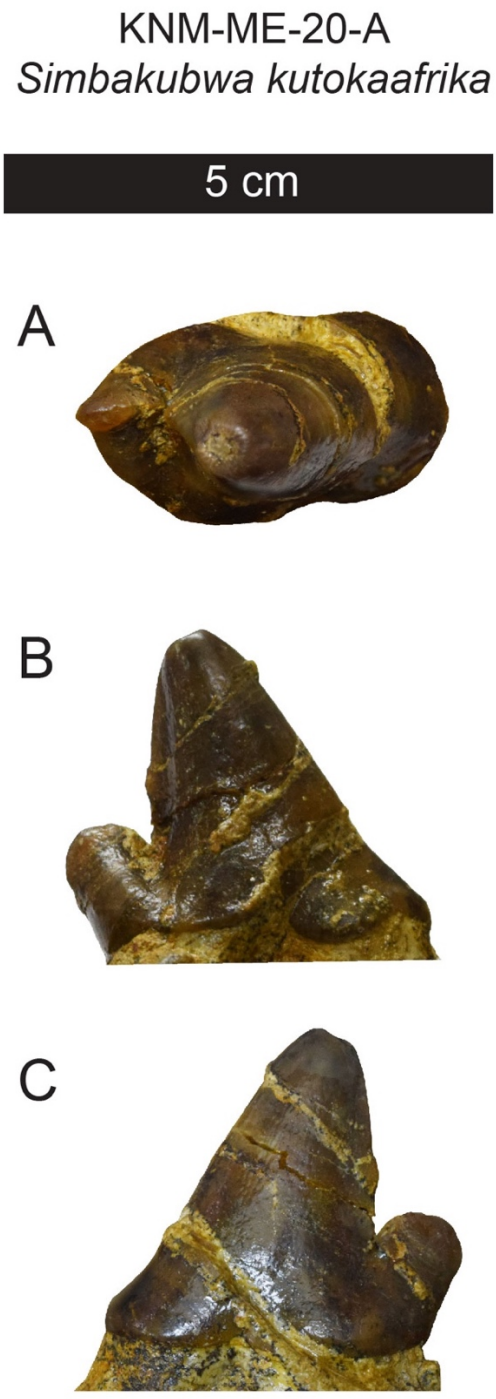

FIGURE 2S. Additional views of *Simbakubwa* holotype left p4 (KNM-ME 20A). **A**, occlusal view; **B**, lingual view; **C**, buccal view. The images of p4 in Fig. 1 show this tooth slightly skewed due to the distorted preservation of the specimen. These views are provided to clarify the proportions of the tooth in standard dental views. Note the sectorial hypoconid and buccolingually compressed postprotocristid. 3D rendering of the specimen is also accessible as part of Project 483 at <www.morphosource.org>. Scale bar is 5 cm.

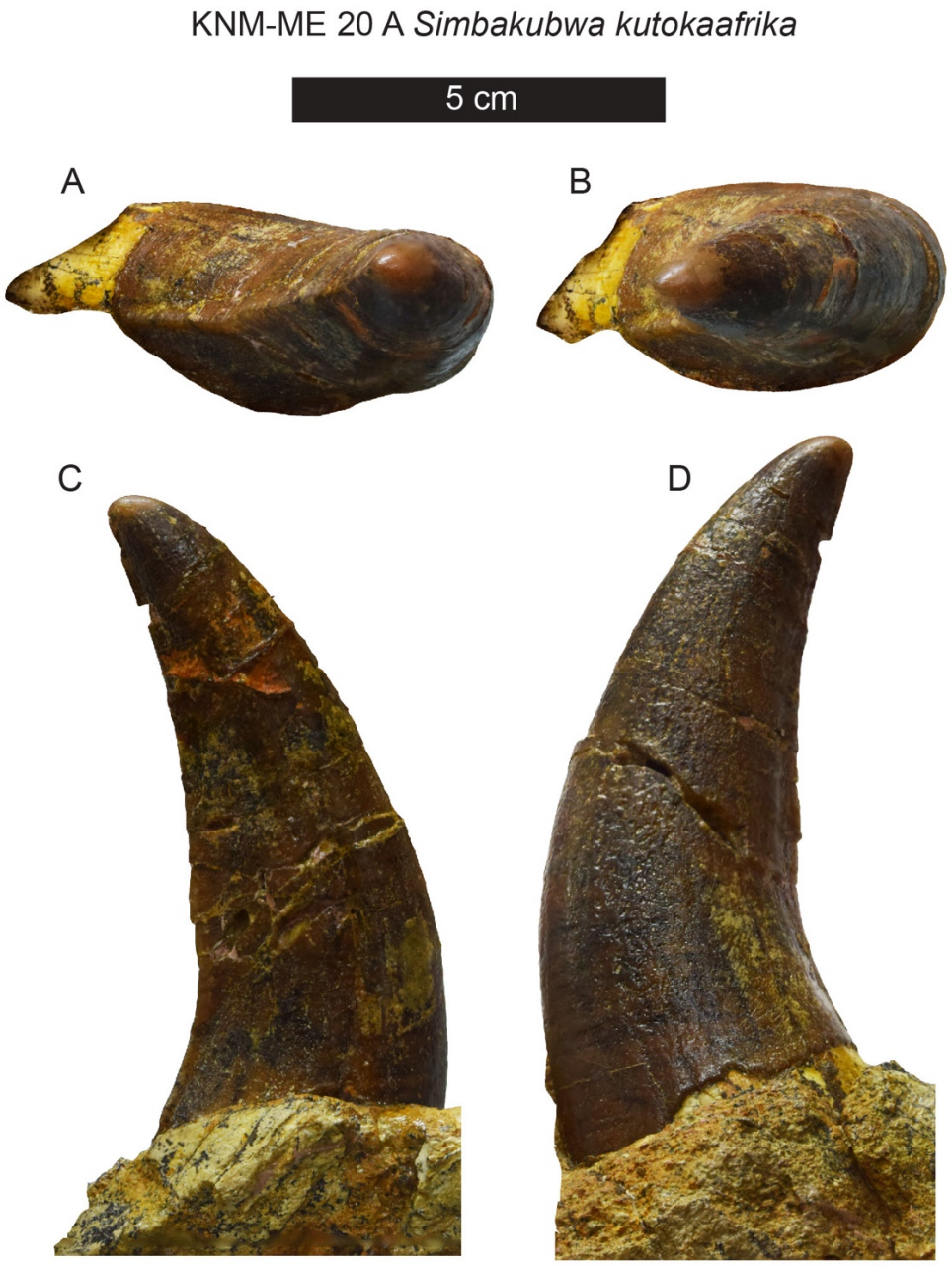

FIGURE 3S. Additional views of *Simbakubwa* holotype left canine (KNM-ME 20A). **A**, occlusal-distal view; **B**, occlusal-mesial view; **C**, lingual view; **D**, buccal view. The holotype dentary of *Simbakubwa* is preserved with the mesial portion of the dentary out of alignment with the distal portion, creating some skew in the proportions of the canine and p4. These additional views are provided to clarify the proportions of the canine in standard orientations. 3D rendering of the specimen is also accessible as part of Project 483 at <www.morphosource.org>. Scale bar is 5 cm.

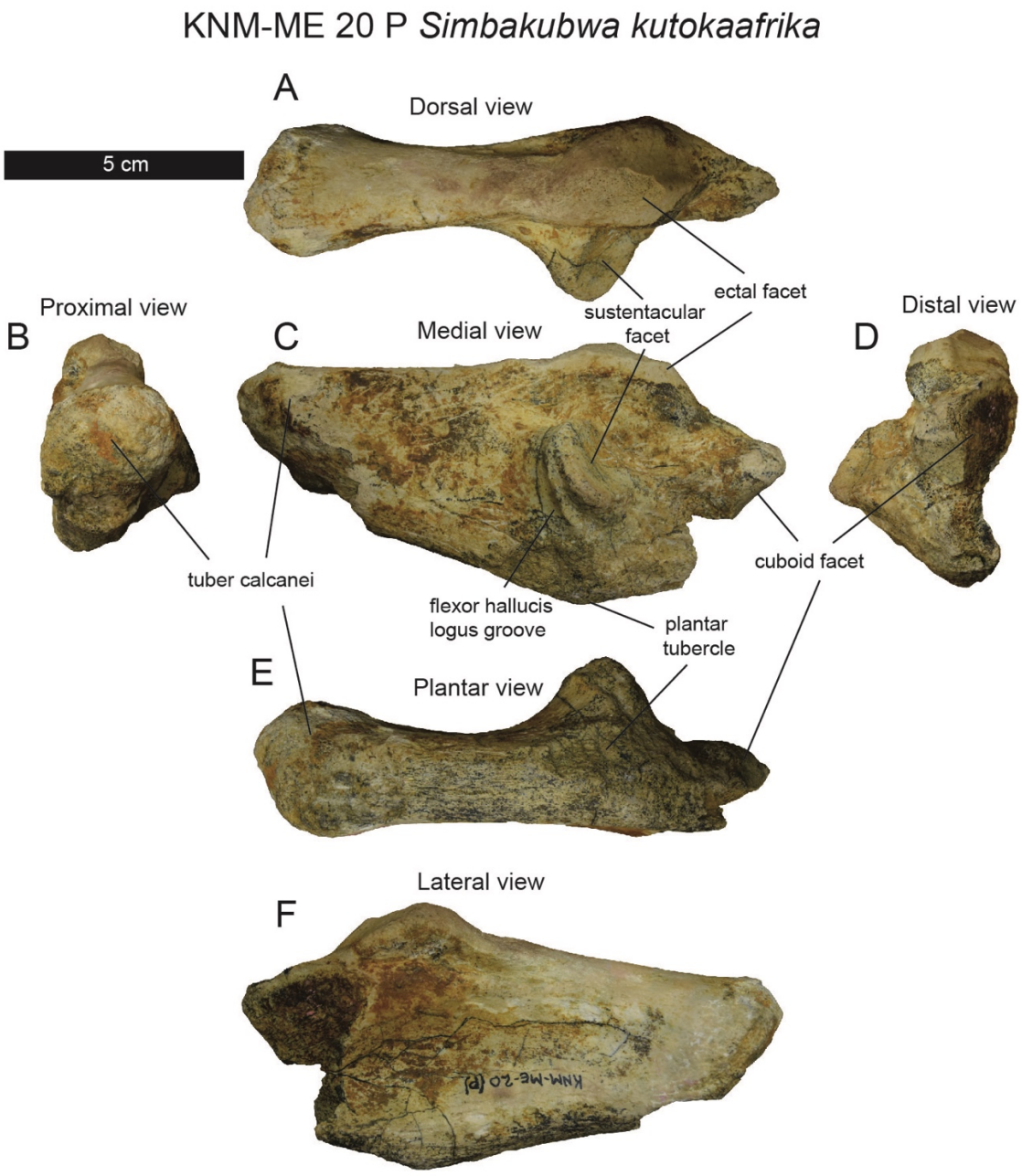

FIGURE 4S. Additional views of *Simbakubwa* calcaneum (KNM-ME-20P). **A**, dorsal view; **B**, proximal view; **C**, medial view; **D**, distal view; **E**, plantar view; **F**, lateral view. The specimen is part of Fig. 7 and these additional views of the specimen are provided to further clarify the morphology and proportions of the specimen. 3D rendering of the specimen is also accessible as part of Project 483 at <www.morphosource.org>. Scale bar is 5 cm.

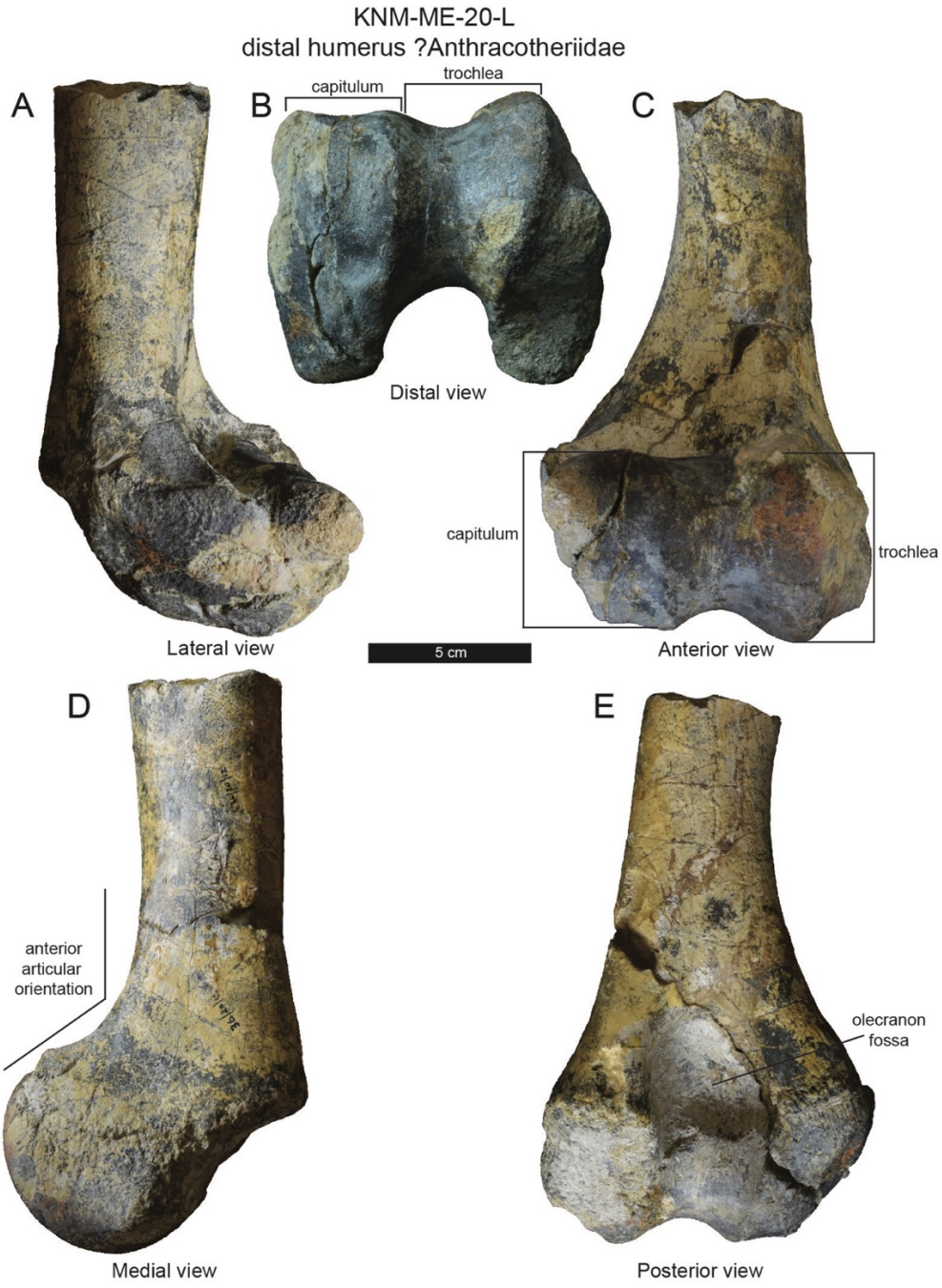

FIGURE 5S. Meswa Bridge ?Anthracotheriidae right humerus (KNM-ME 20L). This specimen was collected in proximity to *Simbakubwa kutokaafrika* and is shown in **A**, lateral view; **B**, distal view; **C**, anterior view; **D**, medial view, and; **E**, posterior view. Historically the specimen has been associated with the holotypic material of *S. kutokaafrika* and it was given the same accession number (KNM-ME 20). However, based on comparisons to humeri referred to Anthracotheriidae (Fig. S8) and to *Hyainailouros sulzeri* (Fig. S7), we tentatively refer this specimen to Anthracotheriidae. See the main text for anatomical comparisons. 3D rendering of the specimen is also accessible as part of Project 483 at <www.morphosource.org>. Scale bar is 5 cm.

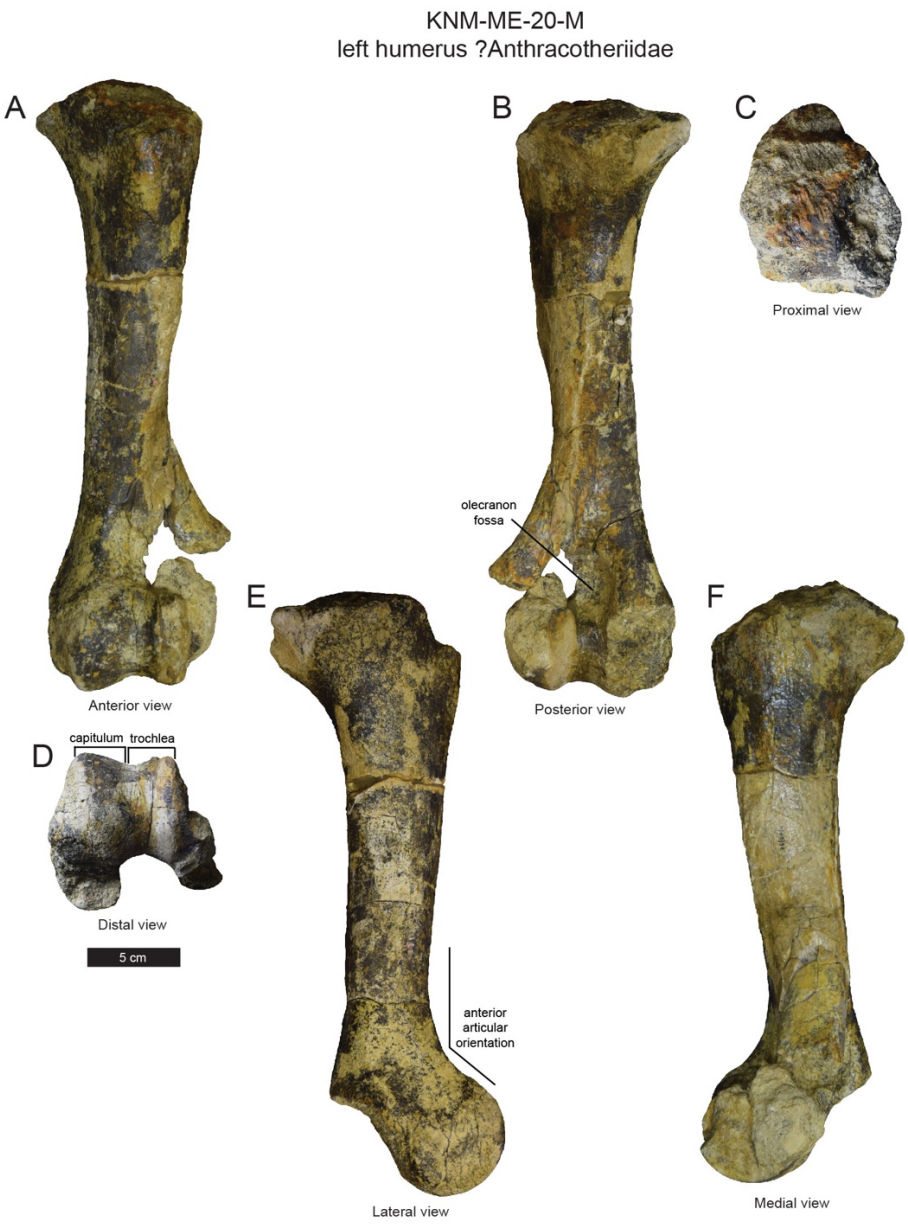

FIGURE 6S. Meswa Bridge ?Anthracotheriidae left humerus (KNM-ME 20M). This specimen was collected in proximity to *Simbakubwa kutokaafrika* and is shown in **A**, anterior; **B**, posterior view; **C**, proximal view; **D**, distal view, and; **E**, lateral view; and medial view. Historically the specimen was associated with the holotypic material of *S. kutokaafrika* and it was given the same accession number (KNM-ME 20). However, based on comparisons to humeri referred to Anthracotheriidae (Fig. S8) and to *Hyainailouros sulzeri* (Fig. S7), we tentatively refer this specimen to Anthracotheriidae. See the main text for anatomical comparisons. Note the cylindrical capitulum and the anterior projection of the distal articulation. Though it appears there is a supratrochlear foramen, this is an artifact of the reconstruction of the specimen. Based on the material preserved superior to the capitulum, it appears there was a deep olecranon fossa that did not perforate the entire distal humerus. This olecranon fossa morphology is shared with Anthracothereiidae and not with *H. sulzeri*. 3D rendering of the specimen is also accessible as part of Project 483 at <www.morphosource.org>. Scale bar is 5 cm.

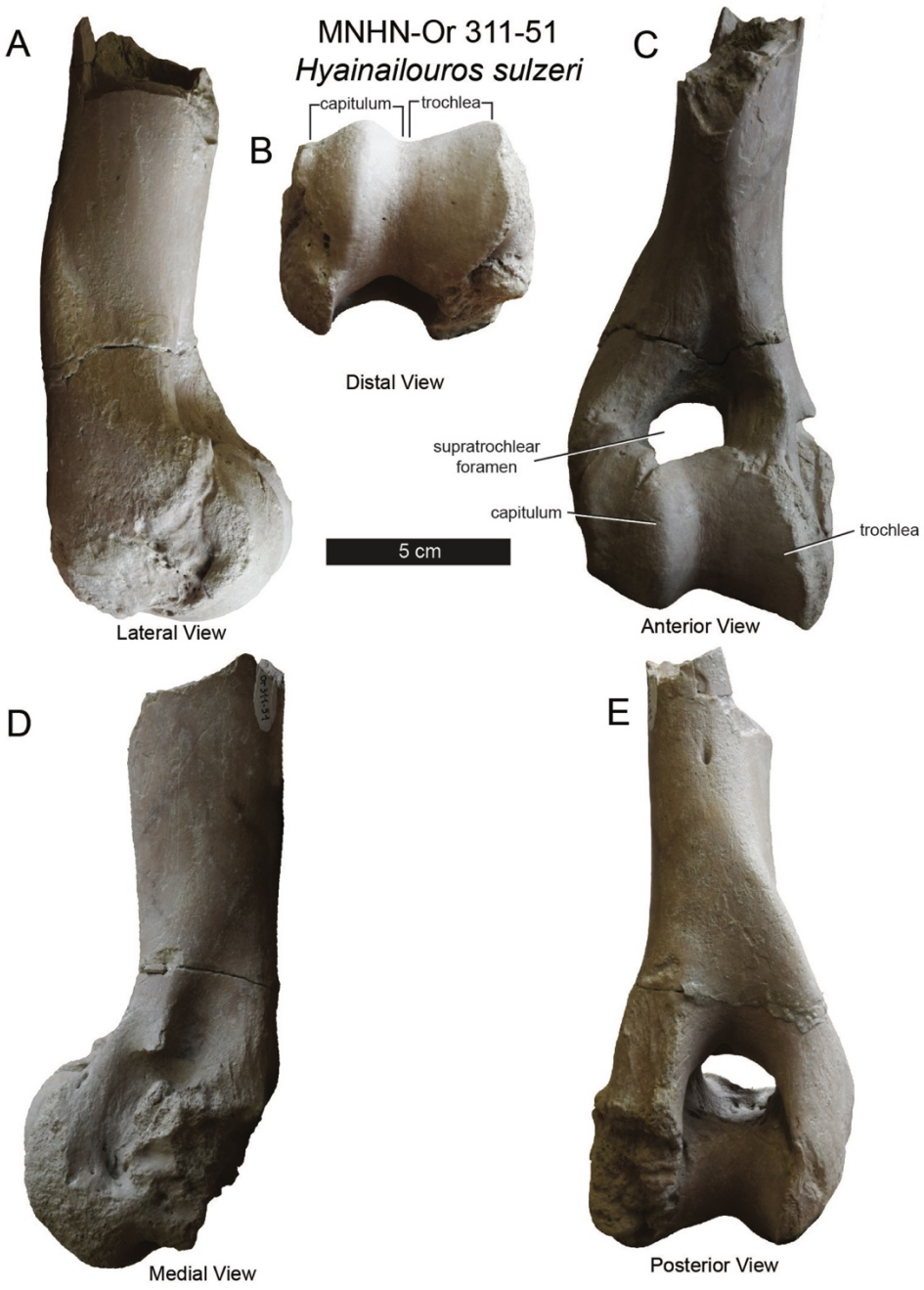

FIGURE 7S. *Hyainailouros sulzeri* right humerus (MNHN.F.Or 311-51). Distal humerus referred to *H. sulzeri* by Ginsburg (1980) in **A**, lateral view; **B**, distal view, **C**, anterior view, **D**, medial view, **E**, and posterior view. Though *Hyainailouros* and *Simbakubwa* are from distinct lineages, both are united in Hyainailourinae and shared a common ancestor in the late Oligocene. It is likely the forelimb of *Simbakubwa* more closely resembled the forelimb of *Hyainailouros* than the humeri found along with the holotype of *Simbakubwa* at Meswa Bridge (Fig. S5 and Fig. S6). See the main text for further discussion of anatomical features that distinguish the Meswa Bridge humeri from *Hyainailouros* and possibly unites the Meswa Bridge specimens with Anthracotheriidae. Scale bar is 5 cm.

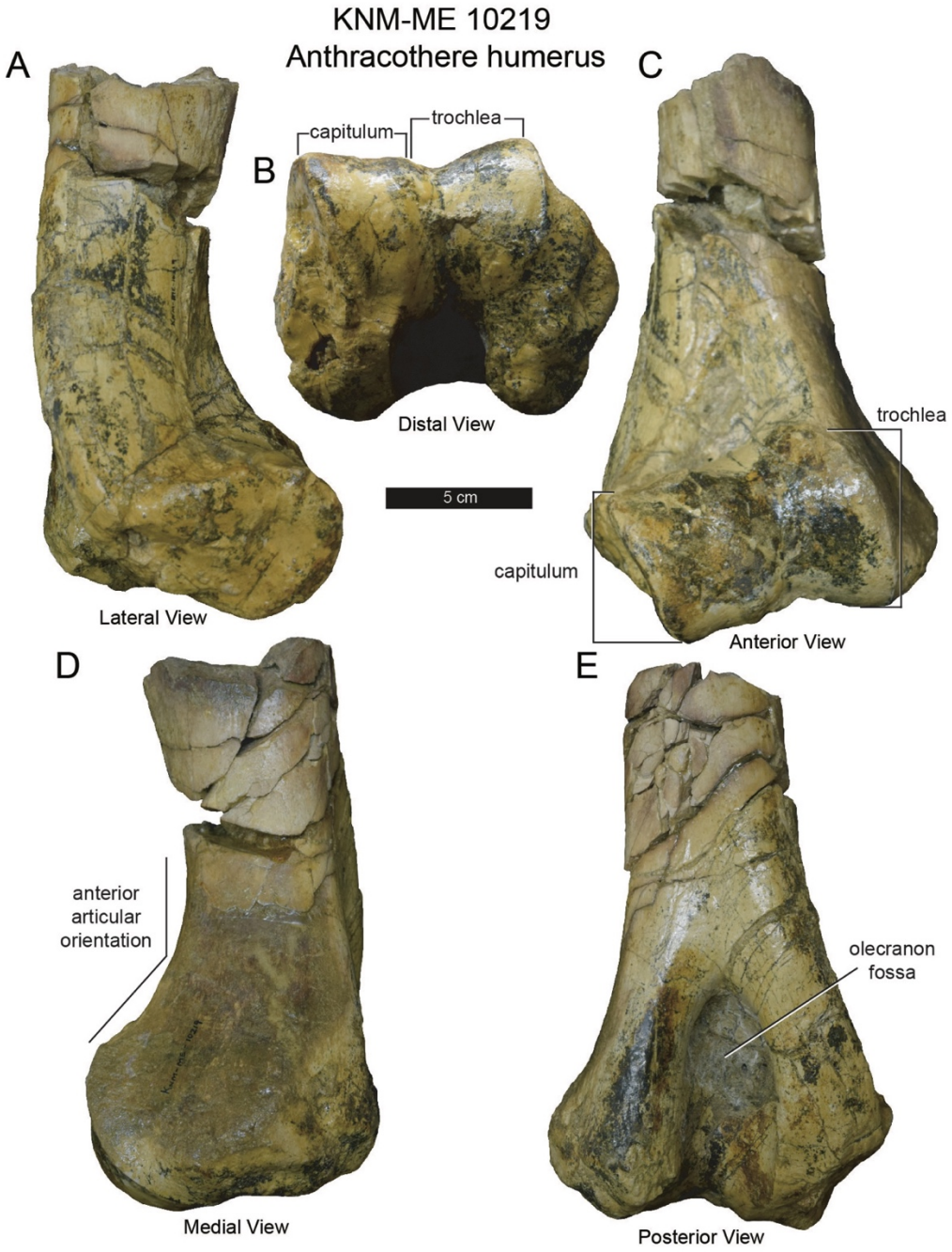

FIGURE 8S. Meswa Bridge Anthracotheriidae right humerus (KNM-ME 10219). **A**, lateral view; **B**, distal view; **C**, anterior view; **D**, medial view; and **E**, posterior view. This specimen was not found in close proximity to the holotype material of *Simbakubwa kutokaafrika* and was referred to Anthracotheriidae. It is illustrated here to provide comparative context for the tentative referral of KNM-ME 20L (Fig. S5) and KNM-ME 20M (Fig. S6) to Anthracotheriidae. Note the mediolaterally elongate, cylindrical capitulum, the anterior projection of the articular condyles, and the deep olecranon fossa. 3D rendering of the specimen is accessible as part of Project 483 at <www.morphosource.org>. Scale bar is 5 cm.

FIGURE 9S. Meswa Bridge ?Anthracotheriidae right ulna (KNM-ME 20K). **A**, lateral view; **B**, anterior view; **C**, medial view. Historically the specimen was associated with the holotypic material of *Simbakubwa kutokaafrika* and it was given the same accession number (KNM-ME 20). However, based on comparisons to ulnae referred to Anthracotheriidae (Fig. S11) and to *Hyainailouros sulzeri* (Fig. S10), we tentatively refer this specimen to Anthracotheriidae. Note the flattened radial notch, the broad and anteriorly facing interosseous margin for articulation with the radius, and the proximally projecting olecranon process with an apparent secondary ossification. It is unclear how much of the distal portion of the ulna is missing. The distal projection is not the styloid process. 3D rendering of the specimen is accessible as part of Project 483 at <www.morphosource.org>. Scale bar is 5 cm.

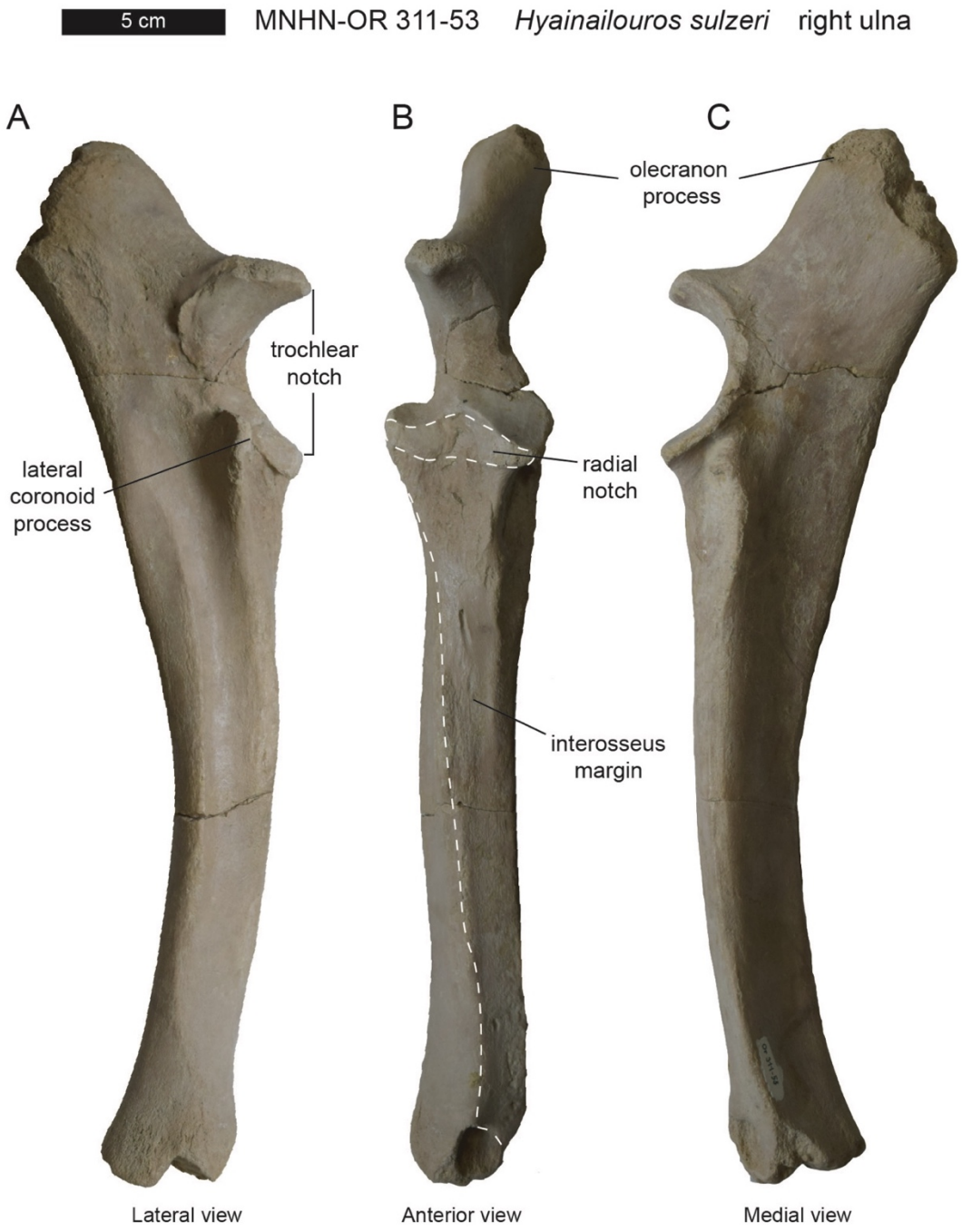

FIGURE 10S. *Hyainailouros sulzeri* right ulna (MNHN.F.Or 311-53). This specimen was referred to *H. sulzeri* by Ginsburg (1980). **A**, lateral view; **B**, anterior view; and **C**, medial view. Like the humerus of *Hyaenodon* (Mellett, 1977), the radial notch is anteriorly positioned, and it is more concave than the radial notch on KNM-ME 20K and KNM-RU 1133 (Anthracotheriidae). The interosseous margin indicates the radius wrapped from the lateral to medial side of the ulna. The olecranon process is posteriorly deflected. Scale bar is 5 cm.

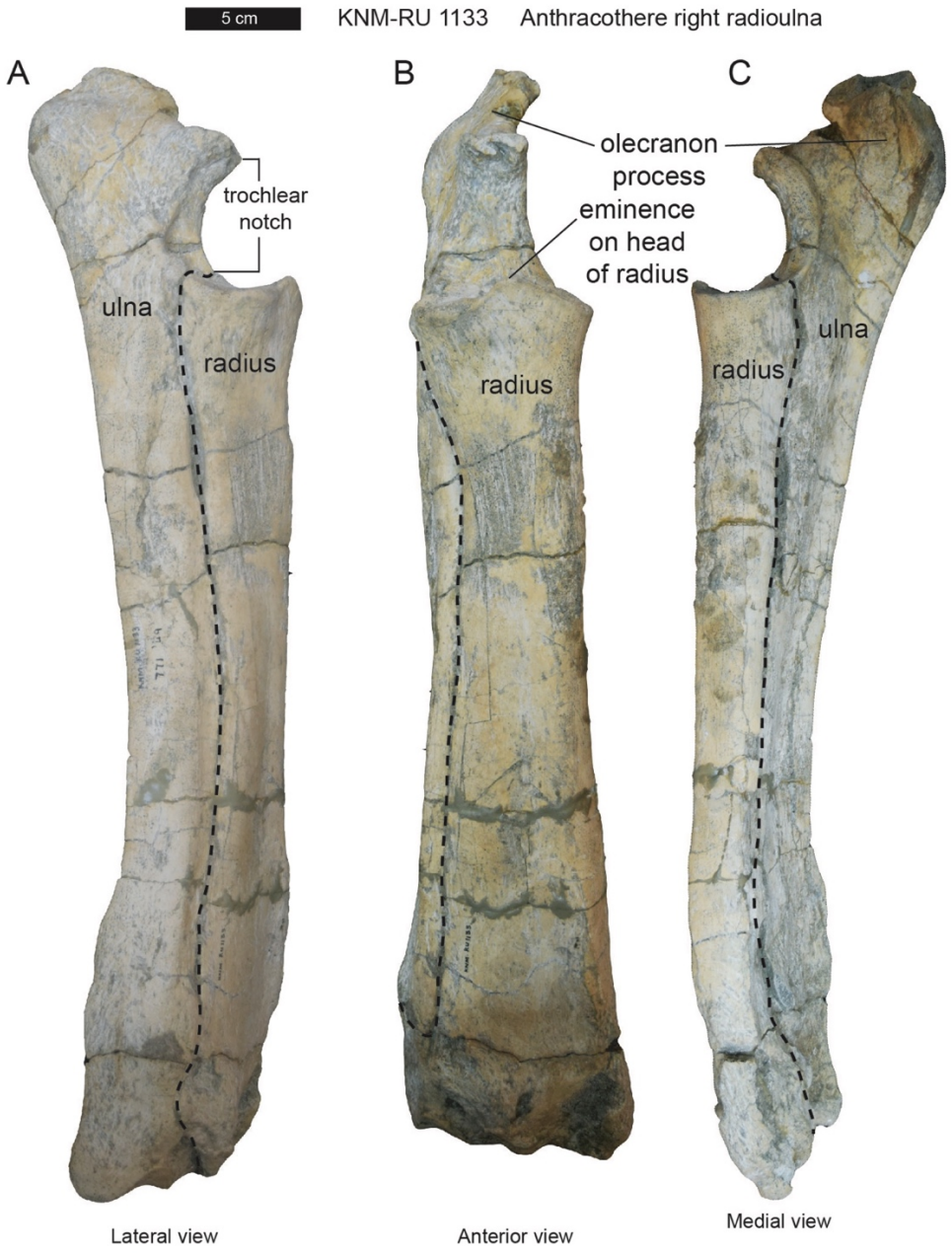

FIGURE 11S. Rusinga Island, Kenya anthracothere right radioulna (KNM-RU 1133). **A**, lateral view; **B**, anterior view; and **C**, medial view. This specimen is from Rusinga Island and is younger than the Meswa Bridge forelimb material referred to Anthracotheriidae (Fig. S5, Fig. S6, Fig. S8, Fig. S12). It shares with KNM-ME 20K a wide, anteriorly oriented radial notch and broad interosseous margin for the radius. It shares with KNM-ME 20J a mediolaterally wide radial corpus and a distinct anterior eminence on the radial head. While the Meswa Bridge material is not fused as it is in the Rusinga Island radioulna, KNM-ME 20K and KNM-ME 20J articulate and lock together in a manner very similar to the fused forelimb referred to Anthracotheriidae. 3D rendering of the specimen is accessible as part of Project 483 at <www.morphosource.org>. Scale bar is 5 cm.

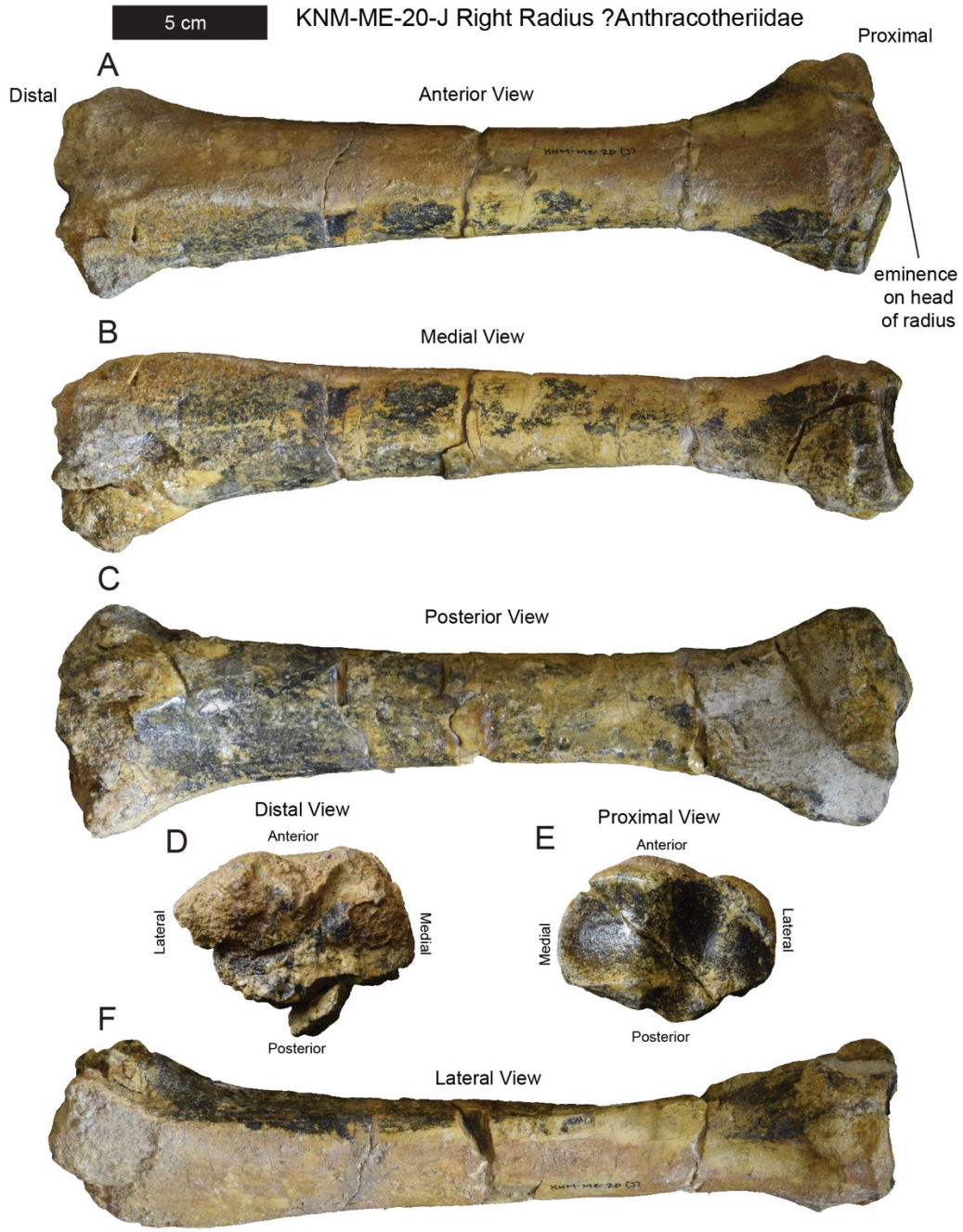

FIGURE 12S. Meswa Bridge ?Anthracotheriidae radius (KNM-ME 20J). **A**, anterior view; **B**, medial view; **C**, posterior view; **D**, distal view; **E**, proximal view; **F**, and lateral view. Historically the specimen was associated with the holotypic material of *Simbakubwa kutokaafrika* and it was given the same accession number (KNM-ME 20). However, based on comparisons to radii referred to Anthracotheriidae (Fig. S11) and to *Hyainailouros sulzeri* (Fig. S13), we tentatively refer this specimen to Anthracotheriidae. Compared with *H. sulzeri*, the Meswa Bridge radius is mediolaterally wider and more columnar. Like the anthracothere radioulna from Rusinga Island, Kenya (Fig. S11) the radial head bears a distinct midline eminence and a broad posterior articulation for with the ulna. Scale bar is 5 cm.

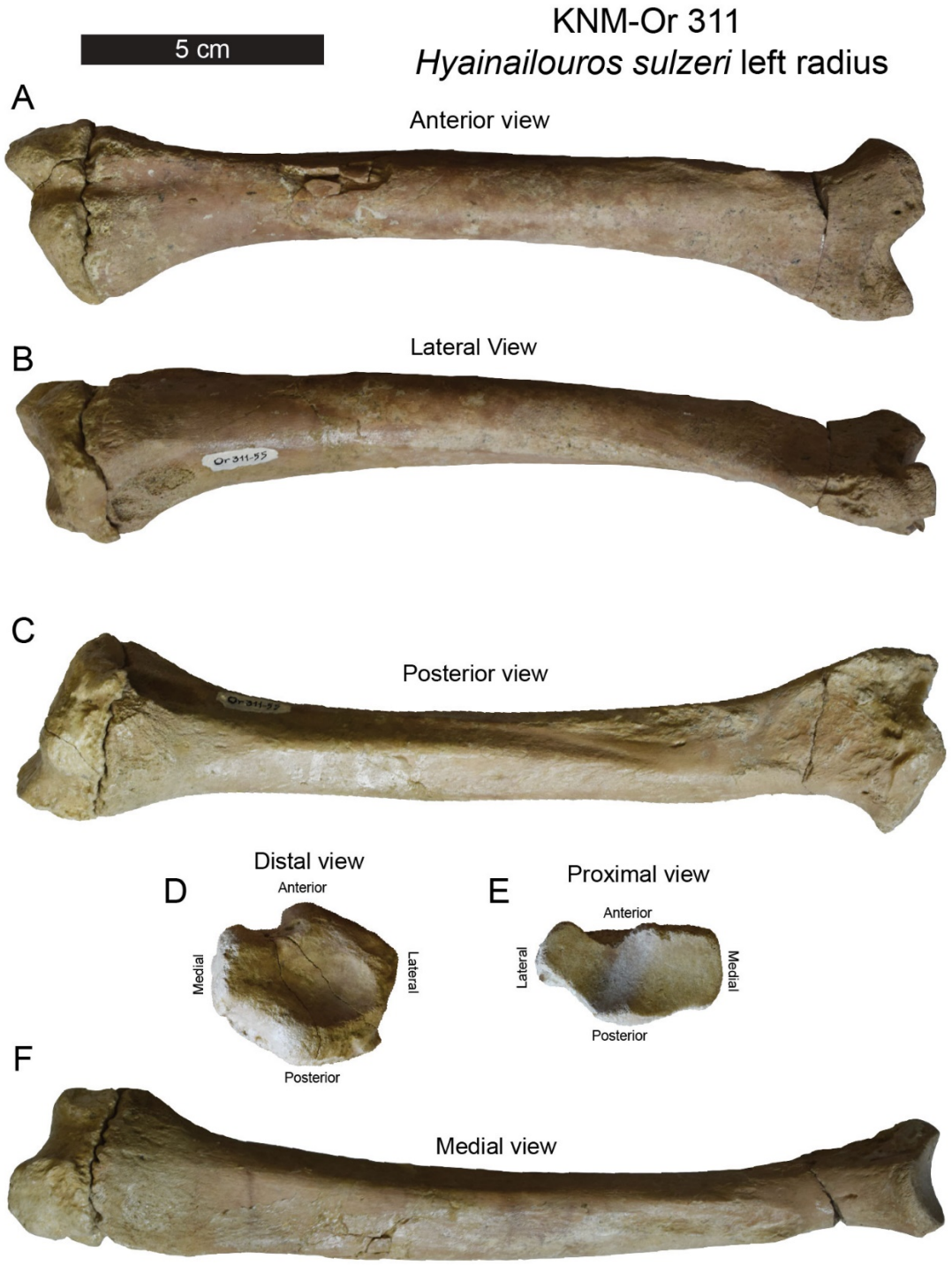

FIGURE 13S. *Hyainailouros sulzeri* left radius (MNHN.F.Or 311-55). Specimen described by Ginsburg (1980) in **A**, anterior view; **B**, lateral view; **C**, posterior view; **D**, distal view; **E**, proximal view; and **F**, medial view. Note the radius referred to *H. sulzeri* is more anteroposteriorly compressed than the Meswa Bridge radius (Fig. S12) and the radial shaft is curved rather than columnar. Scale bar is 5 cm.

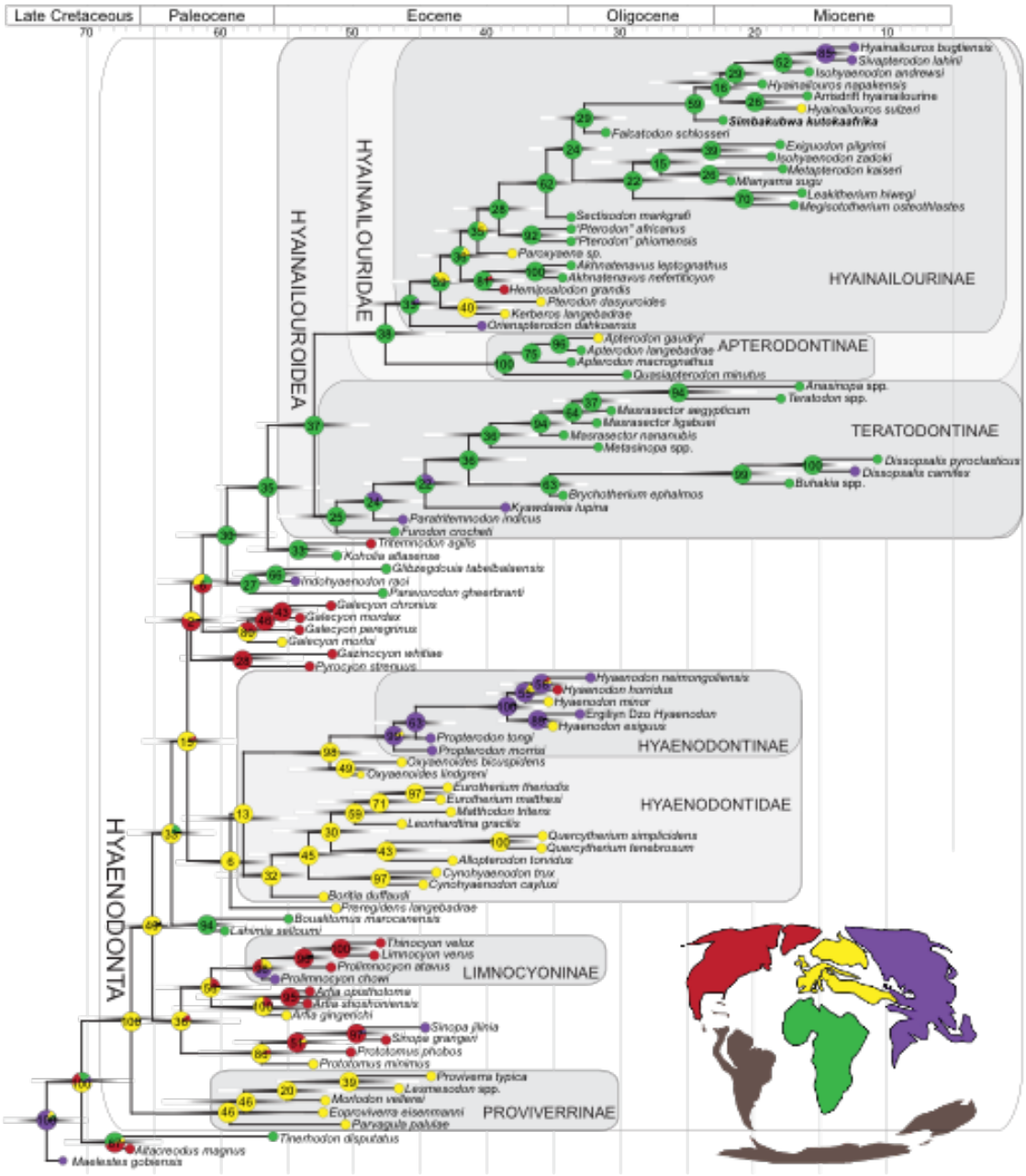

FIGURE 14S. *Simbakubwa kutokaafrika* 'allcompat' consensus tree in color. Same figure as Fig. 9 only using color rather than greyscale. Summarized results of the Bayesian "tip-dating" analysperformed using 94 OTUs and 156 morphological characters. Divergence dates and terminal ages reflect the median age estimate for the taxon or node. Pie charts indicate relative support for ancestral continental area for each node (**green**, Afro-Arabia; **yellow**, Europe; **red**, North America; **purple**, India and Asia; **dark grey**, areas without hyaenodonts) based on BBM biogeographic analysis. Terminal circles indicate continent where OTU was discovered. Posterior probability support shown over biogeography pie chart. Nodal gradient bars represent 95% highest posterior density (HPD) age estimates. BBM results for each node, evolutionary rate estimates, date ranges for each OTU, and non-clock Bayesian analysis used to calibrate the tip-dating clock rate are contained in Supplementary Data.

MORPHOLOGICAL CHARACTERS (156) USED IN PHYLOGENETIC ANALYSIS

The list of 156 morphological characters used for this analysis, including citations for characters drawn from or modified by earlier analyses of hyaenodont systematics.

Lower Dentition

Deciduous Lower Dentition

1) dP_3 paraconid height: paraconid indistinct (0); paraconid present lower than talonid (1); paraconid present and taller than talonid (2).
2) dP_3 protostylid between protoconid and talonid: present (0); absent (1). (New Character relative to Borths and Stevens, 2017)
3) dP_4 paraconid height: lower than half protoconid height (0); half protoconid height or taller (1).
4) dP_4 metaconid height: lower than half paraconid height (0); half paraconid height or taller (1); metaconid absent (2). (compare with Bastl et al. 2014; Character 12)
5) dP_4 talonid basin cusps: Entoconid and hypoconid present (0); Only hypoconid present (1). (compare with Bastl et al. 2014; Character 13)
6) dP_4 talonid length proportion: More than 1/3 length of entire tooth (0); less than 1/3 length of entire tooth (1).

Adult Lower Dentition

7) First mental foramen position: inferior to P_1 (0); inferior to P_2 (1). (Solé et al., 2014; Character 0)
8) Second mental foramen position: inferior to P_3 (0); inferior to P_4 (1). (Solé et al., 2014; Character 1)
9) P_1: present (0); absent (1). (Solé et al., 2014; Character 2)
10) P_1 root number: two roots (0); one root (1). (Polly, 1996; Character 13; Zack, 2011; Character 2; Solé et al., 2014; Character 2)
11) P_2 talonid mesiodistal length: absent to short (0); elongate with distinct inflection separating postprotocristid from talonid (1). (modified Polly, 1996; Character 3; Egi et al., 2005; Character 34; Solé et al., 2014; Character 5)
12) P_2 to P_3 relative mesiodistal length: P_2 shorter than P_3 (0); P_2 as long or longer than P_3 (1). (Egi et al., 2005; Character 29; Solé et al., 2014; Character 6)
13) P_3 inclination: perpendicular to horizontal ramus, tooth forms isosceles triangle in buccal view (0); tooth inclines distally, preprotocristid mesially convex (1).
14) P_3 buccolingual width relative to mesiodistal length: width 33% of length (0); width 50% of length (1); width more than 50% of length (2).
15) P_3 paraconid morphology: absent or small (0); developed with distinct postparacristid (1). (modified Polly, 1996; Character 6; Egi et al., 2005; Character 35; Solé et al., 2014; Character 7)
16) P_3 talonid mesiodistal length: short, cusp-like (0); long, distinct inflection separating postprotocristid from talonid (1). (modified Polly, 1996; Character 4; Egi et al., 2005; Character 37; Solé et al., 2014; Character 8)
17) P_3 entoconid: absent (0); present (1). (Solé et al., 2014; Character 9)

18) P_3 to P_4 relative mesiodistal length: P_3 shorter than P_4 (0); P_3 as long or longer than P_4 (1). (Egi et al., 2005; Character 31; Solé et al., 2014; Character 10)
19) P_4 inclination: perpendicular to horizontal ramus, tooth forms isosceles triangle in buccal view (0); tooth inclines distally, preprotocristid mesially convex (1).
20) P_4 orientation: talonid and protoconid aligned with horizontal ramus (0); talonid and protoconid at oblique angle to horizontal ramus (1). (New Character relative to Borths and Stevens, 2017)
21) P_4 paraconid morphology: present but poorly developed (0); paraconid well-developed (1); paraconid indistinct to absent (2). (modified Polly, 1996; Character 7; Solé et al., 2014; Character 11)
22) P_4 metaconid: absent (0); present, usually weakly developed or ridge-like (1). (modified Solé et al., 2014; Character 12)
23) P_4 entoconid: absent (0); present (1). (Solé et al., 2014; Character 14)
24) P_4 hypoconulid: present and distinct (0); absent or indistinct from entoconid (1). (New Character relative to Borths and Stevens, 2017)
25) P_4 hypoconid height: short, less than 33% of protoconid height (0); tall, more than 33% protoconid height (1). (modified Solé et al., 2014; Character 16)
26) P_4 talonid basin: buccolingually compressed and shallow (0); buccolingually wide and deep (1); absent (2).
27) P_4 precingulid and postcingulid: absent (0); present (1). (modified Solé et al., 2014; Character 18)
28) P_4 relative height: mesiodistally longer than height (0); mesiodistally shorter than height (1); mesiodistal length and height subequal (2).
29) P_4 height relative to molars: shorter than all molars (0); taller than M_1 only (1); taller than M_2 (2).
30) P_5 presence: present (0); absent (1).
31) M_1 and M_2 entoconid morphology: well developed or bulbous (0); crestiform with visible apex (1); undifferentiated entocristid (2). (modified Zack, 2011; Charcter 23; Solé et al., 2014; Character 27)
32) M_1 and M_2 talonid depth: deep (0); shallow (1). (modified Zack, 2011; Character 25; Solé et al., 2014; Character 29)
33) M_2 entocristid in lingual view: parallels hypocristid (0); present, stops before metaconid (lower than hypocristid) (1); weak ridge or absent (2).
34) M_3 entocristid: parallels hypocristid (0); present, stops before metaconid (lower than hypocristid) (1); weak ridge or absent (2).
35) M_1 and M_2 talonid buccolingual width: narrow, less than 80% width of trigonid (0); wide, greater than 80% trigonid (1). (modified Solé et al., 2014; Character 28)
36) M_1 mesiodistal length relative to M_2: M_1 length subequal or longer than M_2 (0); M_1 length less than M_2 (1). (modified Zack, 2011; Character 26; Solé et al., 2014; Character 31)
37) M_1 relative to M_2 mesiodistal length: M_1 greater than or equal to M_2 trigonid length (0); M_1 greater than M_2 paraconid length (1); M_1 equal to or shorter than M_2 paraconid length (2). (New Character relative to Borths and Stevens, 2017)
38) M_1–M_3 trigonid height relative to talonid: trigonid tall on all molars, talonid less than 50% of trigonid height (0); trigonid low on all molars, talonid more than 50% of trigonid height (1); trigonid low on M_1 and M_2 (2). (modified Solé et al., 2014; Character 32)

39) M_3 postprotocristid distal trend in buccal view: slopes mesial to distal (0); perpendicular to alveolus (1); slopes distal to mesial (overhangs talonid) (2).
40) M_2 cristid obliqua orientation relative to mesiodistal axis: lingual to buccal trend (0); parallel to mesiodistal axis (1); buccal to lingual trend (2). (compare to Zack, 2011; Character 21)
41) M_2 and M_3 paraconid position relative to protoconid, angle defined relative to mesiodistal axis of mandible: directly mesial to protoconid,15 degrees (0); slightly lingual paraconid, 15.1 to 45 degree angle (1); strong lingual position, 45.1 to 60 degrees (2). *Ordered*
42) M_3 postparacristid mesial to distal trend: steep slope to preprotocristid ("V" shaped acute angle) (0); shallow slope to preprotocristid (forms right angle with preprotocristid) (1); forms obtuse angle with preprotocristid (2). *Ordered*
43) M_2 and M_3 paraconid height relative to protoconid: paraconid significantly shorter than protoconid (0); paraconid slightly shorter than protoconid (1); paraconid and protoconid subequal in height (2).
44) M_3 postparacristid to premetacristid in lingual view: postparacristid shorter than premetacristid (0); postparacristid subequal to premetacristid (1); postparacristid longer than premetacristid (2).
45) M_3 postparacristid length to preprotocristid in buccal view (carnassial blade proportions): postparacristid much shorter than preprotocristid (30%) (0); postparacristid half length of preprotocristid (1); postparacristid more than half preprotocristid length (2); subequal lengths (3).
46) M_2 and M_3 metaconid expression: connate and connects to paraconid base (0); connate, separated from paraconid (1); fold or ridge (2); absent (3). *Ordered*
47) M_1 metaconid: taller than paraconid (0); subequal to paraconid (1); shorter than paraconid or absent (2). *Ordered* (compare to Polly, 1996; Character 18)
48) M_2 metaconid: taller than paraconid (0); subequal to paraconid (1); shorter than paraconid or absent (2). *Ordered* (compare to Polly, 1996; Character 18)
49) M_3 metaconid: taller than paraconid (0); subequal to paraconid (1); shorter than paraconid or absent (2). *Ordered* (compare to Polly, 1996; Character 19)
50) M_2 mesiodistal length to M_3 length: M_2 shorter than M_3 (0); M_2 subequal to M_3 (1); M_2 longer than M_3 (2); M_3 absent (3). *Ordered* (compare to Zack, 2011; Character 30)
51) M_2 talonid mesiodistal length (% of total mesiodistal length): >40% (0); 40% to 30% (1); 29% to 21% (2); <20% (3). *Ordered*
52) M_3 talonid mesiodistal length (% of total mesiodistal length): >40% (0); 40% to 30% (1); 29% to 21% (2); <20% (3). *Ordered*
53) M_3 talonid: present, bears hypoconid and hypoconulid (0); present, only one distinct cusp (1); absent (2). *Ordered*
54) M_2 buccal talonid margin: steep slope distal to mesial (0); shallow slope distal to mesial (1); parallel to alveolus (2); slopes mesial to distal (3). *Ordered*
55) M_3 buccal talonid margin angle from highest point to lowest: steep slope distal to mesial (0); shallow slope distal to mesial (1); parallel to alveolus (2); slopes mesial to distal (3). *Ordered*
56) M_1–M_3 ectocingulid: weakly expressed to absent (0); distinct (1). (modified Solé et al., 2014; Character 34)
57) M_1–M_3 postcingulid: absent (0); present (1). (modified Solé et al., 2014; Character 35)
58) M_1–M_3 ectocingulid to postcingulid connection: separated (0); fused (1). (modified Solé et al., 2014; Character 36)
59) M_3 talonid buccolingual width relative to M_2 talonid width: equal (0); narrower (1).

60) Mandible inflection anterior to angular process (Solé et al., 2015): present (0); absent (1).
61) Angular process morphology: distinct process with medial inflection (0); gently curved process in line with mandibular corpus (1); ventral inflection (2).
62) Mandibular condyle position: superior to M_3 alveolus (0); directly distal to M_3 alveolus (1); inferior to M_3 alveolus (2).
63) Coronoid process shape: tall, anterior and posterior slopes similar (0); tall, posterior slope concave (1); low, rounded (2).
64) Anterior coronoid angle relative to horizontal ramus: near vertical, 90 to 100 degrees (0); slight posterior inclination, 100 to 110 degrees (1); strong posterior inclination, greater than 110 degrees (2).
65) Masseteric fossa depth: deeply excavated with strong anterior angle, inferior margin well-defined (0); rounded anterior margin, little inferior definition (1); deep fossa but poorly defined inferior margin (2).

Upper Dentition

Deciduous Upper Dentition

66) dP^3 parastyle mesiodistal length: more than half metastyle length (0); less than half metastyle length (1).
67) dP^3 metacone-paracone fusion: metacone distinct cusp (premetacrista slopes to metacone apex; See *Pterodon dasyuroides*) (0); metacone fused to paracone (premetacrista sub-horizontal; See *Apterodon*) (1).
68) dP^3 paracone morphology: pre- and postparacrista similar in slope (apex isosceles triangle in buccal view) (0); preparacrista distally inclined (apex closer to right triangle in buccal view) (1).
69) dP^3 metastyle notch: Small inflection between postmetacrista and metastyle (0); deep notch between postmetacrista and metastyle (1).
70) dP^3 Protocone prominence: mesiodistal length shorter than buccolingual width (narrow) (0); mesiodistal length equal to or longer than buccolingual width (wide) (1). (modified from Bastl et al. 2014; Character 2)
71) dP^3 lingual cingulum: present (distinct lingual connection between parastyle and protocone) (0); absent (faint or no connection between parastyle and protocone) (1). (modified from Bastl et al. 2014; Character 4)
72) dP^4 main cusp height: paracone taller than metacone (0); Paracone subequal to metacone (1); Paracone shorter than metacone (2). *Ordered* (Modified from Bastl et al., 2014; Character 6)
73) dP^4 protocone orientation: Protocone projects mesially to parastyle margin (0); Protocone projects lingually and does not align with parastyle (1).
74) dP^4 ectoflexus: Deep and distinct inflection between metacone and metastyle (0); Indistinct or shallow inflection between metacone and metastyle (1).

Adult Upper Dentition

75) Upper incisor count: 3 or more (0); 2 or fewer (1).
76) Lateral-most upper incisor: incisiform, similar to mesial incisor (0); caniniform (1).

77) Upper canine alveolar cross-section: distally tapers with mesiodistal axis more than 20% buccolingual axis (0); rounded with mesiodistal axis less than 20% buccolingual axis (1). (New Character relative to Borths and Stevens, 2017)
78) P^3 lobe of the protocone or protocone alveolus: absent (0); present but small and alveolus merged lingual alveoli (1); protocone well-developed, individuated and alveolus distinct from lingual alveoli (2). (modified Polly, 1996; Character 9; Egi et al., 2005; Character 4; Solé et al., 2014; Character 39; modified relative to Borths and Stevens, 2017)
79) P^3 root number: two roots (0); three roots (1). (Solé et al., 2014; Character 40)
80) P^3 contact with P^4 parastyle: P^3 contacts or aligned with P^4 parastyle (0); P^3 framed by P^4 parastyle (1).
81) P^4 parastyle: distinct (0); very reduced to absent (1). (modified Egi et al., 2005; Character 8; Zack, 2011; Character 34; Solé et al., 2014; Character 41)
82) P^4 protocone alignment: transversely aligned with paracone (0); mesially shifted relative to paracone (1). (Zack, 2011; Character 36; Solé et al., 2014; Character 42)
83) P^4 protocone morphology: bulbous and distinct from paracone (0); weak separation from paracone, shelf to cingulum-like (1). (modified Polly, 1996; Character 10; Egi et al., 2005; Character 6/7; Solé et al., 2014; Character 43)
84) P^4 metastylar blade (=postmetacrista): short (0); elongate (1). (modified Egi et al., 2005; Character 9; Zack, 2011; Character 35; Solé et al., 2014; Character 45)
85) P^4 metastyle contact with M^1: P^4 metastyle braced buccally by M^1 parastyle (0); P^4 metastyle contacts mesial aspect of M^1 parastyle (1).
86) M^1 and M^2 metastyle blade curvature: straight with carnassial notch (0); postmetacrista arcuate, no carnassial notch (1). (Zack, 2011; Character 42; Solé et al., 2014; Character 46)
87) M^1 and M^2 metastyle blade length: short, carnassial blade shorter than postmetacrista (0); intermediate, subequal to slightly longer than postmetacrista (1); elongate, greater than 1.5x length of postmetacrista (2). *Ordered* (Egi et al., 2005; Character 21; Solé et al., 2014; Character 47)
88) M^1 and M^2 metastyle robusticity (length divided by width): robust or 1.0 or greater (0); moderate or between 0.71 and 0.99 (1); gracile or 0.70 or less. (New Character relative to Borths and Stevens, 2017)
89) M^1 postmetacrista to metastyle angle: Angle less than 130 degrees (0); Angle between 131 and 144 degrees (1); Angle greater than 145 degrees (2).
90) M^1 mesiodistal length relative to M^2: M^1 subequal or longer than M^2 (0); M^1 shorter than M^2 (1). (modified Solé et al., 2014; Character 50)
91) M^1 and M^2 premetaconule crista: present (0); absent (1). (modified Solé et al., 2014; Character 51)
92) M^1 and M^2 conules: metaconule and paraconule present (0); only paraconule present (1); metaconule and paraconule absent (2) (modified Solé et al., 2014; Character 53)
93) M^1 and M^2 precingulum and postcingulum: absent (0); present (1). (modified from Polly, 1996; Character 20; Egi et al., 2005; Character 26; Solé et al., 2014; Character 54)
94) M^1 and M^2 precingulum and postcingulum connection: separated (0); fused lingually (1). (Solé et al., 2014; Character 55)
95) M^1 and M^2 protocone morphology: Triangular, mesial and distal margins angled (0); parallel mesial and distal margins (1). (modified Egi et al., 2005; Character 14)

96) M^1 protocone position relative to paracone and metacone: centered (0); directly lingual to the parastyle (1); mesial to the parastyle (2). *Ordered* (modified Egi et al., 2005; Character 15; Solé et al., 2014; Character 56; State 2 added to Borths and Stevens, 2017)
97) M^1 protocone lingual projection, measured as the ratio of the protocone buccolingual length divided by the length of the bases of the paracone and metacone: long, ratio greater than 0.9 (0); intermediate, ratio between 0.9 and 0.61 (1); short, ratio less than 0.6 (2).
98) M^1 and M^2 metacone mesiodistal length relative to paracone: shorter (0); subequal (1); longer (2). (modified Egi et al., 2005; Character 12)
99) M^1 and M^2 metacone coronal cross section: circular (0); ovoid, slightly compressed buccolingually (1); ellipsoid, strong buccolingual compression (2).
100) M^2 paracone compression: conical, rounded base (0); ovoid (slight buccolingual compression) (1); ellipsoid (strong buccolingual compression) (2).
101) M^1 and M^2 paracone and metacone separation: separated to base (0); fused between base and half of height (1); almost completely fused (2). *Ordered* (modified Polly, 1996; Character 28; Egi et al., 2005; Character 10; Zack, 2011; Character 40)
102) M^1 and M^2 paracone height: paracone taller than metacone (0); paracone as tall as metacone (1); paracone shorter than metacone (2). *Ordered* (modified Egi et al., 2005; Character 11; Zack, 2011; Character 41; Solé et al., 2014; Character 48)
103) M^1 and M^2 protocone height: shorter than paracone/metacone separation (0); same height as paracone/metacone separation (1); subequal to paracone/metacone apices (2). (compare to Zack, 2011; Character 49)
104) M^2 parastyle: absent (0); present and shelf-like (1); present, single distinct cusp (2); present multiple distinct cusps (3). (modified from Egi et al., 2005; Character 19 and Borths and Stevens, 2017)
105) M^1 parastyle compared to M^2: M^1 parastyle relatively shorter than M^2 parastyle (0); parastyle on M^1 and M^2 similar (1).
106) M^1 and M^2 buccal cingulum: absent (0); weak ridge along metastyle base (1); prominent shelf forms shallow basin between metastyle and cingulum (2). (modified Egi et al., 2005; Character 16/17)
107) M^2 ectoflexus: strong, strong indentation (0); weak, slight curve (1); absent, straight (2). (modified Egi et al., 2005; Character 18)
108) Ectoflexus depth on M^1 and M^2: M^1 ectoflexus shallower than M^2 (0); same relative depth between M^1 and M^2 (1); M^2 lacks metastyle (no ectoflexus) (2). *Ordered* (compare to Zack, 2011; Character 52)
109) M^3 metacone: present (0); absent (1). (modified Polly, 1996; Character 15; Zack, 2011; Character 53; Solé et al., 2014; Character 58)

Cranial Characters

110) Nuchal crest morphology: medial to lateral trend from apex to mastoid (0); dorsolateral margin tapers medially with thin connection to exoccipital (1); lateral margins trend medially, very weak ridge connects to exoccipital (2). *Ordered* (modified Polly, 1996; Character 35)
111) Facial wing of the lacrimal: extensive (larger than orbit diameter) (0); moderate (slightly longer than orbit diameter) (1); reduced (shorter than orbit diameter) (2). (modified Polly, 1996; Character 36)

112) Foramen rotundum size: slightly larger than foramen ovale (0); much larger than foramen ovale (1). (Polly, 1996; Character 39)
113) Palatal rugosity or torus at distal margin of palate: well-expressed (0); smooth (1).
114) Zygomatic arch contact: short contact between zygomatic and squamosal (0); extensive contact between zygomatic and squamosal (1).
115) Superior squamosal morphology: superior and inferior margins parallel (0); torsion along superior margin (1).
116) Foramen ovale orientation: anterior orientation (0); palatal orientation (1).
117) Exoccipital condyle position: tall, lateral placement around foramen magnum (0); ventral placement around foramen magnum (1).
118) Notch between occipital condyles: ring-like with no rostral excavation (0); rounded indentation with condyles meeting medially below foramen magnum (1); deep excavation with occipital "processes" following notch (2).
119) Postmandibular process: vertical orientation (0); strong anterior curvature (1).
120) Posterior orbital process: present, strong expression (0); present, weak with frontal "peaked" (1); absent (2).
121) Frontal furrow: absent or indistinct (0); present and well-defined (1).
122) Palatine and pterygoid medial contact: parallel posterior to palatine torus (0); palatines trend medially or partially fuse (1); fused entire extent of palatines (2).
123) Pterygoid size: broad, ventral projection anteriorly extensive (0); short anterior extent, trends medially (1).
124) Frontoparietal suture in dorsal view: steep constriction (0); gentle curvature (1).
125) Lateral expansion of the mastoid process (Solé et al., 2015): projects to midpoint of mandibular fossa (0); projects beyond mandibular fossa (1).
126) Mastoid/paroccipital process: short tubercle (0); well-defined, prong-like process (1).
127) Process at maxilla/jugal suture (Solé et al., 2015): present (0); absent (1).
128) Squamosal constriction in dorsal view: present, squamosal does not extend laterally (0); absent, squamosal expanded laterally (1).
129) Squamosal ventral projection: same transverse plane as petrosal (0); ventral to petrosal (1).
130) Posterior braincase: broad lateral expansion (0); narrow (1).
131) Subarcuate fossa morphology (Polly, 1996): cup-shaped (see *Pterodon*) (0); shallow and horseshoe-shaped (see *Hyaenodon*) (1).
132) Bridge of the stylomastoid foramen primitivum: absent or slender (0); robust (1); roofed over with secondary stylomastoid foramen (2). (Polly, 1996; Character 40)
133) Mastoid sinus lateral to foramen stylomastoid primitivum: absent (0); present (1). (Polly, 1996; Character 41)
134) Ridge of bone dividing posterior petrosal sinus from foramen stylomastoid primitivum (Polly, 1996): present (0); reduced to absent (1). (Polly, 1996; Character 42)
135) Posterior petrosal sinus: absent (0); small (1); greatly inflated (2). (Polly, 1996; character 43)

Postcrania

Humerus

136) Humerus cross-section above brachial flange: triangular (0); rounded (1). (Polly, 1996; Character 44)
137) Brachial flange expression: medium (0); enlarged (1); reduced (2). (Polly, 1996; Character 47)
138) Entepicondylar foramen: present, rounded (0); present, elongate (1); absent (2).
139) Medial epicondyle: large (bulbous) (0); reduced (elongate) (1).
140) Capitulum morphology: rounded, clearly separated (0); cylindrical (1).
141) Greater tubercle of the humerus: prominent, taller than humeral head (0); subequal to height of humeral head (1).

Ulna

142) Proximal trochlear notch orientation: lateral position on shaft (0); medial position on shaft (1).
143) Radial notch orientation: curved and faces laterally (0); flattened and faces anteriorly (1). (Polly, 1996; Character 47)
144) Olecranon process length: longer than trochlear notch (0); subequal or shorter than trochlear notch (1).
145) Olecranon process orientation: projects medially (0); projects ventrally (1).

Femur

146) Third trochanter of femur: large (0); small (1). (modified Polly, 1996; Character 50)

Astragalus

147) Astragalar foramen: large (0); reduced (0). (Polly, 1996; Character 51)
148) Astragalar condyles divided by: shallow depression (0); well-defined fossa or groove (1)
149) Astragalar condyle orientation: oblique relative to astragalar neck (0); parallel to astragalar neck (1).
150) Astragalar head relative to condyles: horizontal orientation (0); slight vertical orientation (1). (Polly, 1996; Character 53)
151) Sustentacular facet connection to astraglar head: clearly separated from astragalar head (0); grades into articulation of astragalar head (1).
152) Sustentacular facet position on astragalar neck: plantar astragalar neck (0); medial astragalar neck (1).

Calcaneum

153) Peroneal tubercle: distinct and separated from cuboid facet (0); part of a flange that grades to cuboid facet (1).
154) Cuboid facet inclination: perpendicular to calcaneal neck (0); plantar inclination (1).
155) Calcaneal neck trend: dorsal and plantar margins parallel (0); tapers proximally to calcaneal tuberosity (1).

156) Astragalar facet angle: oblique orientation to calcaneal neck (0); parallels calcaneal neck (1). (modified Polly, 1996; Character 58)

OTU DATE AND SPECIMEN DATA USED FOR PHYLOGENETIC ANALYSIS

The section presents a list of each specimen scored for the phylogenetic analyses, the absolute time range used for the Bayesian tip-dating analysis, and the sources for the date range.

Akhnatenavus leptognathus
Formation: Jebel Qatrani Formation
Locality: Quarry A, lower Sequence
Geological Age: Rupelian, Oligocene
Absolute Age: 33.9–33.7 Ma
Country: Fayum, Egypt
Citation: Seiffert, 2010; Holroyd, 1999
Specimens observed: AMNH 13263 (Holotype), dentary with P_3–M_3; AMNH 12391, cast of maxilla, P^2–M^2

Akhnatenavus nefertiticyon
Formation: Jebel Qatrani Formation
Locality: L-41
Geological Age: late Priabonian, latest Eocene
Absolute Age: 35–33.9 Ma
Country: Egypt
Citation: Holroyd, 1994; Seiffert, 2010; this study
Specimens observed: CGM 83735 (Holotype), cranium with C, P^2–M^3; DPC 13518, maxilla with M^1; DPC 18242, cranium with P^2–M^2; DPC 7765, dentary with P_2–M_3; DPC 15250, dentary with P_2, P_3, M_2

Allopterodon torvidus
Formation: Fissure fill, between Bouxwiler and Lissieu levels zone
Locality: Egerkingen
Geological Age: MP 14, Lutetian
Absolute Age: 42.6–42.8
Country: Switzerland
Citation: Hartenberger, 1970; Lange-Badré, 1984; Polly and Lange-Badré, 1993; Becker, Rauber, & Scherler, 2013
Specimens observed: NMB En 522 (Holotype), rostrum with P^3–M^3; NMB En 172, dentary with M_2–M_3 (erupting); UCMP 140644 (cast of Egerkingen specimen), dentary with P_1–M_3; NMB En. 167, maxilla with P^4–M^3; NMB Em. 16, partial cranium with P^4–M^3; NMB Bchs 482, palate with P^4–M^3; NMB Eh 557, dentary with P_4–M_3

***Altacreodus magnus* (*Cimolestes magnus*, Lillegraven 1969)**
Formation: Ravenscrag Formation, Frenchman Formation, Hell Creek Formation, Scollard Formation, Lance Formation
Locality: Saskatchewan, Alberta, Montana, Wyoming
Geological Age: Late Cretaceous (?Judithian–"Endmontonian")

Absolute Age: 70–65 Ma
Country: North America
Citation: Lillegraven, 1969; Kielan-Jaworowska et al., 2004; Moore et al., 2014; Fox, 2015
Specimens from Fox, 2015: UALVP 620 (Holotype), dentary with P_4–M_3; UALVP 3793, maxilla with P^4–M^3; UALVP 3267, left M^2; UALVP 3791, dentary with P_3, P_4, M_1–M_3; UALVP 3754, dentary with P_1, P_3, P_4, M_1–M_3;
Specimens from Lillegraven, 1969, Fig. 35 (UALVP 4085b, dP^4; UALVP 3795, canine; UALVP 2997, P^4; dP^3, dP^4; UALVP 3736, M^3, UALVP 3793, maxilla with P^4–M^3), Fig. 36 (UALVP 3676, lower canine; UALVP 3152, P_1; UALVP 3791, P_1–M_3), Fig. 37 (UALVP 3267, M^2; UALVP 3781, P^4; UALVP 3754, P_1, P_3–M_3)

***Anasinopa* spp.**
Formation: Hiwegi Formation and Kulu Formation
Locality: Rusinga Island, Lake Victoria (Maboko Island, Rousing Site 106, Karugu, Mfwanganu Island)
Geological Age: Burdigalian, Miocene
Absolute Age: 17.8–15 Ma
Country: Kenya
Citation: Savage, 1965; Werdelin, 2010
Specimens observed: NHMUK PV M 19081a (Holotype), maxilla with P^4, M^1; NHMUK PV M 19081b (Holotype), maxilla with M^1–M^3; NHMUK PV M 19081c (Holotype), dentary with P_1–M_3; NHMUK PV M 19081d (Holotype), dentary with M_2, M_3; NHMUK PV M 19081e, dentary with canine and P_4; KNM-FT 15092, isolated M^1; KNM-WK 17061, dentary with P_2–M_3; KNM-WK 16992, dentary with M_2; KNM-WK 18197, isolated teeth P^4, M^3, M_2, femoral head, long bone shaft; KNM-RU 52250, dentary with I_1–M_3; KNM-RU 2935, dentary with M_1–M_3; KNM-RU 2928, M^2; KNM-RU 2929, right M^2; KNM-FT 3658, M_1

Apterodon gaudryi (=A. flonheimensis; =A. intermedius)
Formation: Quercy, Mainz Basin, Weisselter Basin
Locality: Espenhain
Geological Age: Late Rupelian (MP22), Early Oligocene
Absolute Age: 32.6–30.9 Ma
Country: Germany
Citation: Lange-Badré and Böhme, 2005; Grohé et al., 2012
Specimens observed: AMNH 12391 (Cast of Holotype), P_4–M_3; BSPG 2008.43 (*Apterodon intermedius* holotype), P_4–M_2; NHMUK PV M 55a, maxilla with M^1–M^2

Apterodon langebadreae
Formation: Idam Unit, Sarir Tibisti Basin
Locality: 68.19, 69.53, 25, Dur At-Talah
Geological Age: Late Bartonian
Absolute Age: 39 if Late Bartonian (Grohé et al. 2012); Likely 33 and Rupelian (Seiffert, 2010); range used: 37–33 Ma
Country: Libya
Citation: Grohé et al., 2012; Seiffert, 2010

Specimens observed: NHMUK PV M 85297 (Holotype), dentary with C–M_3; NHMUK PV M 85298 (Holotype), detnary with C, P_2–M_3; NHMUK PV M 85300 (Holotype), maxilla with C, P^1, P^4–M^3; NHMUK PV M 85301, maxilla with I^2–P^2; NHMUK PV M 85303, maxilla with P^3; NHMUK PV M 85304, frontal fragment; NHMUK PV M 85307, squamosal fragment; NHMUK PV M 85308, squamosal fragment; NHMUK PV M 85309, sagittal crest; NHMUK PV M 85310, cranial fragment; NHMUK PV M 85312, occipital fragment; NHMUK PV M 85313, cervical vertebra; NHMUK PV M 85315, femur; NHMUK PV M 85315, distal femur; NHMUK PV M 85317, proximal femur; NHMUK PV M 85318, humerus; NHMUK PV M 85319, proximal tibia; NHMUK PV M 85320, distal tibia; NHMUK PV M 85321, distal radius; NHMUK PV M 85322, ulna; NHMUK PV M 85323, proximal radius; NHMUK PV M 85324, metacarpal IV; NHMUK PV M 85325, distal metacarpal IV; NHMUK PV M 85327, phalanx I; NHMUK PV M 85328, phalanx II; NHMUK PV M 85329, phalanx II, NHMUK PV M 85330, rib; NHMUK PV M 85331, distal fibula; NHMUK PV M 85332, innominate fragment; NHMUK PV M 85333, innominate fragment

Apterodon macrognathus
Formation: Qasr el Sagha Formation, Jebel Qatrani Formation
Locality: Quarry A
Geological Age: Early Rupelian
Absolute Age: 33.9–33.7 Ma
Country: Fayum, Egypt
Citation: Holroyd, 1994; Lewis and Morlo, 2010; Seiffert, 2010
Specimens observed: CGM 8982 (Holotype), dentary with P_2–M_2; AMNH 13236, cranium with I^1–M^3; AMNH 13237, cranium with I^1–M^3; CGM 29916, dentary with P_2–M_3; DPC 7731, maxilla with canine–M^3; UCMP 154454, dentaries with canine–M_3; DPC 7731, maxilla with C–M3; DPC 0959, humerus; DPC 11347, dentary with M_1–M_2; SMNS 12643, dentary with canine–M_3; SMNS 11950 (Holotype), dentary P_4–M_3; SMNS 47724, palate with canine–M^3; SMNS 11267a, dentary with P_4–M_3; SMNS 11267b, dentary with M_3; SMNS 43466, astragalus; SMNS 43467, radius; SMNS 47729, distal humerus, ulnae, tibia; BSPG 1905 XIII 510, dentary with Canine, P_2, P_4–M_3; BSPG 1905 XIII 9, maxilla with P^4–M^3; YPM 18160, dentary with canine, P_4–M_3; AMNH 13240, dentary with canine–M_3; AMNH 13247, tibia; AMNH 92794, calcaneum; AMNH 13241, dentary with P_2–M_3; NHMUK PV M 8441, astragalus; DPC 1143, M^1; DPC 2557, dentary with M_1–M_3; DPC 4126, maxilla fragment with dP^3; DPC 8217, left dentary with dP_3, dP4, M_1.

Arfia gingerichi
Formation: Tienen Formation
Locality: Dormaal
Geological Age: MP7, very close to PETM
Absolute Age: 55.6–55.4 Ma
Country: Belgium
Citation: Smith and Smith, 2001; Smith, Rose & Gingerich, 2006
Specimens observed: IRSNB M1275 Holotype, M_3; IRSNB M1301, P_3; IRSNB M1302, DP_4; IRSNB M1303, P_4; IRSNB M1304, M_1; IRSNB M1305, M_2; IRSNB M1306, M_3; IRSNB M1307, P^3; IRSNB M1358, DP^4; IrSNB M1308, P^4; IRSNB M1309, M^1; IRSNB M1310, M^2; IRSNB M1311, M^3

Arfia opisthotoma
Formation: Willwood Formation
Locality: Clarks Fork Basin, Bighorn Basin, Powder River Basin, Piceance Creek Basin
Geological Age: Early Eocene, early to middle Wasatchian (Sandcouleean Wa2 to late Graybullian Wa5)
Absolute Age: 55–53 Ma
Country: USA
Citation: Matthew, 1901; Ivy, 1993; Gunnell, 1998
Specimens observed: AMNH 99, UM 78996, dentary with M_1–M_3; UM 69949, dentary with canine, P_2–M_3
Specimens from literature: UA 8271, rostrum with canine–M^2 (Gingerich and Deutsch, 1989)

Arfia shoshoniensis
Formation: Willwood Formation
Locality: Clarks Fork Basin, Bighorn Basin, Powder River Basin
Geological Age: Early Eocene, early to middle Wasatchian (early Sandcouleean Wa1 to early Graybullian Wa3)
Absolute Age: 55–53 Ma
Country: USA
Citation: Matthew, 1915; Ivy, 1993; Gunnell, 1998
Specimens observed: AMNH 16158 (Holotype), UM 85935, rostrum with P^1–M^3; UM 75186, dentaries with canine, P_2–M_3; UM 80487, dentary with P_1–M_3; UM 69474, partial skeleton with humeri, vertebral elements, tibia, femora, astragali, calcaneum, metapodials, innominate; UM 75383, radius
Specimens from literature: UM 65502, M^1–M^2, M_2–M_3 (Gingerich and Deutsch, 1989)

Boritia duffaudi
Formation: ?
Locality: La Borie
Geological Age: Early Eocene, MP8 and MP9
Absolute Age: 54–51 Ma
Country: France
Citation: Solé et al., 2014a
Specimen from literature: MHNT.PAL.2010.19.1 (Holotype), P_3, P_4, M_1–M_3

Boualitomus marocanensis
Formation: Sidi Daoui and Recette 4 quarries, lowermost bed I
Locality: Grand Daoui, Ouled Abdoun Basin
Geological Age: earliest Ypresian
Absolute Age: 55.8–54 Ma
Country: Morocco
Citation: Gheerbrant et al., 2006; Seiffert, 2010
Specimens observed from a cast of the holotype: OCP DEK/GE 306 (Holotype), dentary with canine, P_2–M_3 (thanks to E. Gheerbrant for creating the cast)

Brychotherium ephalmos
Formation: Jebel Qatrani Formation
Locality: L-41
Geological Age: late Priabonian, latest Eocene
Absolute Age: 35–33.9 Ma
Country: Egypt
Citation: Holroyd, 1994; Seiffert, 2010; Present study
Specimens studied: CGM 83750 (Holotype), dentary with C–M_3; DPC 17627, dentary with P_4–M_3; DPC 11990, rostrum with P^4M^3; DPC 11569A, dentary with C, P_2–M_3; DPC 11569B, dentary with P_2, P_3, M_1–M_3; DPC 11474, dentary with dP_3, dP_4, M_1, M_2

***Buhakia* spp.**
Formation: Moghra Formation, Karungu,
Locality: Wadi Moghra
Geological Age: early Miocene (Burdigalian)
Absolute Age: 18 Ma – 16.8 Ma
Country: Egypt
Citation: Morlo, Miller & El-Barkooky, 2007; Morales and Pickford, 2017
Specimens: DPC 8974, dentary with dP_4, M_1, M_2 (holotype of *Buhakia moghraesis*); KNM-KA 77, maxilla with P^3, P^4, M^1, M^2, M^3 (*Buhakia* sp. I in Morales and Pickford 2017); GSN AD 241'99, M_2 (holotype of *Buhakia hyaenoides*)

Cynohyaenodon trux
Formation: Wittenberg Formation (among others)
Locality: Geiseltal (Lutetian, MP11; Germany), Egerkingen (Lutetian, ?MP13–Mp14; Switzerland)
Geological Age: Lutetian, MP11–MP14
Absolute Age: 48.6–40.4 Ma
Country: Germany, France, Switzerland
Citation: Solé et al., 2014; Van Valen, 1965; Lange-Badré and Haubold, 1990
Specimens observed: NMB Em 17, dentary with P_2, P_3, P_4, M_1, M_2, M_3; NMB En 187, dentary with M_1, M_2, M_3; NMB En. 111, maxilla fragment with M^1, M^2; GMH 10831, dentary with M_2, M_3; GMH 3986, dentary with M_1, M_2, M_3; GMH 3984, dentary with P_3, P_4, M_1, M_2, M_3; GMH 3985, dentary with dentary P_3, P_4, M_1, M_3; GMH 3987, dentary with P_2, dP_3, dP_4, M_2

Cynohyaenodon cayluxi
Formation: Quercy, Egerkingen
Locality: Quercy, Egerkingen
Geological Age: MP14, MP18–MP20, Priabonian, Late Eocene
Absolute Age: 48–34 Ma
Country: France
Citation: Solé, 2013; Solé et al., 2014b
Specimens observed: MCZ 8901, cranium with P^3–M^3; MCZ 8902, dentary with P_3–M_3; UCMP 140651, dentary with P_2–M_3 (cast); UCMP 140652, dentary with P_2–M_2 (cast); UCMP 140653, dentary with P_2–M_3; MNHM Qu 8562, cranium with P^2–M^3; MNHM Qu 8566, dentary with P_4–

M_3; MNHM Qu 8564, dentary with canine–M_2; MNHM Qu unnumbered, maxilla with P^4–M^3; NHMUK PV M 9612, dentary P_2–M_3

Dissopsalis carnifex
Formation: probably upper part of Kamlial Formation; probably lower Chinji Formation; middle Nagri Formation
Locality: Y592, GSP 6459, YPM 20050 (See Barry, 1988 for discussion)
Geological Age: middle to late Miocene
Absolute Age: at least 16.1–10.7 Ma, possibly 8.8 Ma
Country: Pakistan
Citation: Berry, 1988
Specimens observed: GSP-Y 51401, dentary with alveoli of canine, P_1, P_2, crowns of P_3, P_4, M_1, M_2, and M_3; GSP-Y 20340, maxilla fragment with M^2 and M^3; GSP-Y 30571, M_2; GSP-Y 24296, dentary with dP_2, dP_3, fragments of dP_4, M_1, erupting M_2; AMNH 9895, dentary with P_4 and M_1; AMNH 19401, cranial fragments with P^2, P^3, P^4, M^1, M^2; GSP-Y 41167, astragalus; GSP-Y 23081, calcaneum; GSP-Y 30561, calcaneum.

Dissopsalis pyroclasticus
Formation: Ngorora Formation (Locality 2/56) and Kaboor
Locality: Tentatively in (Lewis and Morlo discussion) Kaboor, Fort Ternan, Maboko, Moroto, Napak
Geological Age: Middle Miocene
Absolute Age: 15–9 Ma
Country: Kenya
Citation: Savage, 1965; Barry, 1988; Lewis and Morlo, 2010; Werdelin, 2010
Specimens observed: NHMUK PV M 19082, dentary with P_4–M_1 (Holotype); KNM-MB 25305, maxilla fragment with M^2; KNM-MJ 13, maxilla fragment with P^4–M^1; KNM-FT 13770, M_3; KNM-MB 8432, M^2; KNM-FT 15092, M^1; KNM-BN 1191, M^2; KNM-FT 3562, dentary with P_2–P_4, M_1–M_2; KNM-FT 3357, maxilla with dP^3–dP^4

Eomaia scansoria
Formation: Yixian Formation
Locality: Liaoning Province
Geological Age: Early Cretaceous, middle Barremian
Absolute Age: 129.7–122.1 Ma
Country: China
Citation: Kielan-Jaworowska et al., 2004; Chang et al., 2009; Beck and Lee, 2014
Specimen scored from Kielan-Jaworowska et al., 2004

Eoproviverra eisenmanni
Formation: Rians
Locality: Rians
Geological Age: earliest Eocene, MP7
Absolute Age: 55.8–48.6 Ma
Country: France
Citation: Godinot, 1981; Solé et al., 2014a

Specimen scored from Literature: From Godinot, 1981: MNHN.F.RI 400, M_2; MNHN.F.RI 203, M_3; MNHN.F.RI 401, M^1; MNHN.F.RI 362, M^2; MNHN.F.RI 2014, dentary with M_1–M_2

Eurotherium matthesi
Formation: Wittenberg Formation (among others)
Locality: Geiseltal (Lutetian, MP11; Germany), Egerkingen y, a+B (Lutetian, ?MP13–Mp14; Switzerland), La Défense (Lutetian, MP13; France), Issel (Lutetian, MP14; France), Aigues-Vives 2 (Lutetian, ?MP13; France)
Geological Age: Lutetian, MP11–MP14
Absolute Age: 48.6–40.4 Ma
Country: Germany, France, Switzerland
Citation: Polly and Lange-Badré, 1993; Solé, Falconnet, and Yves, 2014
Specimens observed: UCMP 140638, dentary with P_1–M_3 (Cast, original specimen number not recorded); UCMP 140639, maxilla with P^2–M^3 (Cast, original specimen number not recorded); UCMP 140635, astragalus (cast of GMH XIV 3614); UCMP 140634, calcaneum (cast of GMH XIV 2364); GMH XIV 224, P_1–M_3; GMH XI-1-1954 (Holotype), dentary with P_2–M_3; GMH XIV-3419-1956, cranium with P^2–M^3; GMH XIV-1357-1955, cranium with P^2–M^3; GMH XIV-3332-1956, dentary with P_3–M_3; GMH XIV-3614-1956, astragalus; GMH XIV-2364-1954, calcaneum

Eurotherium theriodis
Formation: unnamed karst infillings
Locality: Egerkingen y, a+B (Lutetian, ?MP13–Mp14; Switzerland), Aigues-Vives 2 (Lutetian, ?MP13; France)
Geological Age: Lutetian, MP13
Absolute Age: 48.6–40.4 Ma
Country: France, Switzerland
Citation: Polly and Lange-Badré, 1993; Solé, Falconnet, & Yves, 2014
Specimens observed: UCMP 140647, dentary with P_2–M_3 (Cast, original specimen number not noted); NMB Em. 12, cranium with P^1–M^1 (Holotype), NMB Em. 14a, cranium with P^3–P^4, humerus (Egerkingen, 1915 on card); NMB Em. 14b (Paratype), dentary with M_2–M_3; NMB Em. 193 (Paratype), M^2; NMB En. 247, M^2; NMB En. 120, dentary with P_3–M_3; NMB En. 106, P^4; NMB En. 140, M^1; NMB Eh. 536, dentary with M_2–M_3
Observed in Solé et al. (2015): MNHN.F.ERH427, right dentary with canine–M_3; MNHN.F.ERH428, dentary with P_1, P_2, P_4

Exiguodon pilgrimi
Formation: Hiwegi Formation, Kulu Formation
Locality: Rusinga Island (Kavirondo Gulf), Napak
Geological Age: Burdigalian, early Miocene
Absolute Age: 20–15 Ma
Country: Kenya, Uganda
Citation: Savage, 1965; Lewis and Morlo, 2010; Werdelin, 2010
Specimens observed: NHMUK PV M 19100a (Holotype), dentary with P_2–M_3; NHMUK PV M 19100b (Holotype), dentary with P_3–M_3; NHMUK PV M 19100c (Holotype), cervical vertebrae; KNM-RU 259, dentary with P_4–M_3; KNM-RU 2945, dentary with P_2, P_4, M_1; KNM-RU 2943,

P_4, M_2, M_3; KNM-RU 5415, astragalus; KNM-RU 8404, rostrum; KNM-SO 1105, dentary with M_2; KNM-SO 1668, maxilla fragment with P^4–M^1; KNM-SO 5395, M_2; KNM-SO 5671, dentary with M_1–M_3; KNM-SO 8420, dentary with P_4

Falcatodon schlosseri
Locality: Quarry V, possibly Quarry B if AMNH 13262 is included
Geological Age: Rupelian, Oligocene
Absolute Age: 33.9–30 Ma
Country: Egypt
Citation: Holroyd, 1999; Morales and Pickford, 2017
Specimens observed: AMNH 13262, dentary with P_2–M_3; DPC 5664 (holotype), dentary with P_3–M_3; DPC 4877, dentary with P_3–M_3; DPC 5431, maxilla with P^4–M^2

Furodon crocheti
Formation: Glib Zegdou Formation
Locality: HGL 50 and HGL 50 bis, Gour Lazib, Tindouf Province
Geological Age: late Ypresian or middle Lutetian
Absolute Age: 49.3–45.7 Ma
Country: Algeria
Citation: Solé et al., 2014b; Coster et al., 2012
Observed casts of material at MNHM thanks to F. Solé: HGL 50bis-56 (Holotype), dentary with canine base, P_1–P_3 alveoli and P_4–M_3; HGL 50-410, M_1; HGL 50-404, M^1; HGL 50-405, M^1; HGL 50-407, M^1

Galecyon chronius
Formation: Willwood Formation
Locality: Bighorn Basin, Clarks Fork Basin
Geological Age: Wa-6
Absolute Age: 53–50.3 Ma
Country: USA
Citation: Zack, 2011
Observed from Zack (2011): USNM 487920 (Holotype), petrosal, P^3 (left), P^4–M^1; USNM 511004, dentary with P_2, P_4–M_3; YPM 23341, dentary with P_2–P_4; USNM 51190, P_4; USGS 8769, dentary with M_1–M_2; USGS 10284, M_2; USNM 487920, dentary with C, P_2–P_3, M_1–M_3; USGS 15956, M^2
Observed from Zack and Rose (2015): USNM 511004, humerus, ulna, scaphoid, lunate, tibia, astragalus, calcaneum, cuboid

Galecyon mordax
Formation: Willwood Formation
Locality: Bighorn Basin, Clarks Fork Basin
Geological Age: Wa-5, Wa-1/2 to Wa-3
Absolute Age: 55.4–53 Ma
Country: USA
Synonym: *Prolimnocyon robustus*
Citation: Zack, 2011

Specimens observed: UM 85887, dentary with canine, P_2–M_2; AMNH 16157 (Holotype), canine, P_2–M_3
Observed from Zack (2011): USNM 490637, dentary with canine, P_1–M_1
Observed from Gingerich and Deutsch (1989): UM 76227, dentary with M_1–M_3
Observed from Zack and Rose (2015): USNM 1125, glenoid of left scapula; USNM 1125, innominate; USNM 1125, femur, fibula

Galecyon morloi
Formation: Tienen Formation
Locality: Dormaal
Geological Age: MP7, very close to PETM
Absolute Age: 55.6–55.4 Ma
Country: Belgium
Citation: Smith and Smith, 2001; Smith, Rose & Gingerich, 2006
Specimens observed: IRSNB M1314, M_1; IRSNB M1312, DP_4; IRSNB M1313, P_4; IRSNB M1315, M_2; IRSNB M916, M_3; IRSNB M1316, P_4; IRSNB M1317, M^1 or M^2

Galecyon peregrinus
Formation: Willwood Formation
Locality: Bighorn Basin, Clarks Fork Basin, Powder River Basin
Geological Age: early Wasatchian (Sandcouleean), Wa-0 to Wa-1/2
Absolute Age: 55.4–53 Ma
Country: USA
Citation: Zack, 2011
Observed from Zack (2011): USNM 509676 (Holotype), dentary with P_3–M_3; UCMP 217129, M_2; UCMP 217128, M_1

Gazinocyon whitiae
Formation: Green River Basin, Bighorn Basin, Wind River Basin
Locality: Green River Basin, Bighorn Basin, Wind River Basin
Geological Age: Lostcabianian subage, Wasatchian NALMA, early Eocene
Absolute Age: 53–50.3 Ma
Country: Wyoming, USA
Synonym: *Sinopa vulpecula, Prototomus vulpeculus, Gazinocyon vulpecula*
Citation: Matthew, 1915; Gingerich and Deutsch, 1989; Polly, 1996; Rana et al., 2014
Specimens observed: UCMP 137216, dentary with M_3, calcaneum, radius, atlas, axis dens, innominate, ulna, humerus, femur, astragalus, M^2; AMNH 15606, dentary with P_2–M_3
Observed from Gingerich and Deutsch (1989): USNM 19347, maxilla with P^2–M^3

Glibzegdouia tabelbalaensis
Formation: Glib Zegdou Formation
Locality: HGL 10 and HGL 50, Gour Lazib, Tindouf Province
Geological Age: late Ypresian or middle Lutetian
Absolute Age: 49.3–45.7 Ma
Country: Algeria
Citation: Solé et al., 2014b; Coster et al., 2012

Observed casts of material at MNHM thanks to F. Solé: GZC 35 (Holotype), M_2; HGL 10-15, M^2; HGL 50-411, M_1; HGL 50-406, P^3; HGL 50-408, P^3

Hemipsalodon grandis
Formation: Cypress Hills Formation, Clarno Formation, ?Chadron Formation
Locality: Saskatchewan, Oregon, Wyoming, Texas
Geological Age: Late Duchesnean, Bartonian ("late Eocene–early Oligocene" in Mellett)
Absolute Age: 41.2–37.8 Ma
Country: USA
Citation: Mellet, 1969; Solé et al., 2015
Specimens observed: AMNH 95735 (cast of OMSI 619), cranium with I^2–M^3 and dentary with canine, P_3–M_3; AMNH 95736, maxilla with canine, P^3–M^3; AMNH 10636 (cast of NMC 6497, Holotype), dentary with M_3; AMNH 95780 (cast of SDSM 6333), dentary with P_3–M_1

Hyaenodon horridus
Formation: White River Formation, South Dakota (many, see Mellet, 1977)
Locality: Saskatchewan, Wyoming, Montana, Colorado, North Dakota, South Dakota
Geological Age: late Chadronian to late Orellan
Absolute Age: 38–33.3 Ma
Country: USA, Canada
Synonym: *Neohyaenodon horridus, Hyaenodon cruentus*
Citation: Mellet, 1977
Specimens observed: AMNH 39438, cranium with I^1–M^2; AMNH 39439, cranium with I^2, I^3, dC, P^1, P^2 (erupting), dP^3, dP^4, M^1, M^2 (erupting), dentary with canine, P_2, dP_3, dP_4, M_1, M_2; UM 6792, humerus; UM 6786, humerus; AMNH 75704, I^1–M^2, dentary with I_1–M_3; AMNH 1488, cranium with I^2–M^2; AMNH 9809, innominate, sacrum, lumbar vertebrae, femur, tibia, fibula, metapodials, astragalus, ; AMNH 1381, humerus, astragalus, calcaneum; AMNH 75701, humerus, scapula; AMNH 1381, humerus, ulna; AMNH 1175, ulna; MCZ 17395, cranium with I^1–M^2, mandible with I_1–M_3 (dentary occluded to cranium); MCZ 4739, cranium with I^1–M^2 and mandible (occluded) with I_1–M_3; UCMP 22788, cranium with P^1–M^2; UCMP 158793, cranium with I^3–M^2; AMNH unnumbered specimen, cranium, dentaries, skeleton; AMNH 8775, cranium and dentaries (occluded), cervical vertebrae, thoracic vertebrae (T1–T4); YPM 10010, cranium with canine, P^2–M^2, mandible with I_2–M_3; YPM 10916, articulated pes; YPM 10996, humerus; YPM 11035, ulna; YPM 12656 (*Hyaenodon (Neohyaenodon)* holotype), cranium with I^2–M^2 and mandible (occluded) with I_2–M_3; AMNH 75725, dentary with dP_3, dP_4, M_1, M_2; AMNH 97780, dentary with P_2, dP_3, dP_4, M_1, M_2

Ergiliyn Dzo *Hyaenodon*
Formation: Ergiliyn Dzo Formation
Locality: Khoer Dzan and Ergiliyn Dzo localities (?)
Geological Age: early Oligocene
Absolute Age: 34–32 Ma
Country: Mongolia
Citation: Lavrov, 1999; Morlo and Nagel, 2006

Specimens observed: PIN 3110-5785, dentary with I_1–M_3; PIN 3109-283, maxilla with P^2–P^3; PIN 3110-578a, cranium with I^1–M^2, humerus, tibia, femur, radius; PIN 3109-83, maxilla with P^2–P^3

Hyaenodon exiguus
Formation: Euzet-les-Bains (Gard): lower Ludien
Locality: Quercy
Geological Age: late Eocene, Euzet Level Zone, Priabonian
Absolute Age: 37.2–33.9 Ma
Country: France
Citation: Lange-Badré, 1979
Specimens observed: MNHM Qu 8364, dentary with canine, P_4–M_3; MNHM Qu 8593, basicranial fragment with auditory bulla; MNHM Qu 8425, P_4–M_3; MNHM Qu 8647, maxilla fragment with P^3–M^2; MNHM Qu 17662, cranium with erupting teeth exposed dP^2, dP^3, dP^4, P^2, P^3, P^4, M1, M^2; NHMUK PV M 2353, dentary with P_1, dP_3, dP_4, M_1; NHMUK PV M 2353A, dentary with dP_3, dP_4; NHMUK PV M 4498, P_2, dP_4

Hyaenodon minor
Formation: Euzet-les-Bains (Gard): lower Ludien
Locality: Fons 4 (Gard); Quercy; Roc de Santa, Spain; Hordle, lower and upper Headon Beds, England; Gosgen Kanal, Switzerland
Geological Age: late Eocene, Euzet Level Zone, Priabonian
Absolute Age: 37.2–33.9 Ma
Country: France, Spain, England, Switzerland
Citation: Lange-Badré, 1979
Specimens observed: MNHM Qu 8649, cranium with P^1–M^2; MNHM Qu 8461, maxilla fragment with P^1; MNHM QU 8470, maxilla with P^4–M^2; MNHM Qu 8407, M^2; MNHM Qu 8406, M^1; MNHM Qu 8471, dentary with P_3–M_3; MNHM Qu 8429, dentary with P_3–M_3; MNHM Qu 8557, dentary with canine–P_3; MNHM Qu 8450, dentary with P_2–P_4; MNHM Qu 8419, dentary with M_1–M_3; MNHM Qu 8329, rostrum with P^2–M^2; MNHN.F.Qu 9981, astragalus

Hyaenodon neimongoliensis
Formation: Ulantatal Formation
Locality: Ulantatal, Alxa Zuoqi, Nei Mongol
Geological Age: early Oligocene, Hsandagolian
Absolute Age: 33.9–23.03 Ma
Country: China
Citation: Huang et al., 2002; Rodrigues et al., 2014
Specimens observed: IVPP V12438 (Holotype), dentary with canine, P_2–M_3; IVPP V12439, maxilla with P^4–M^2; IVPP V12440, dentary with canine, P_2, P_3; IVPP V12441, P_2

Hyainailouros bugtiensis
Formation: Locality IDs Y0048, Y0051, Y0711, Y0303, Y0336, Y0758, Y0750, Y0504, S0002, S0013, S0015
Locality: Siwaliks

Geological Age: middle Miocene
Absolute Age: 13.7–11.3 Ma
Country: Pakistan
Citation: Flynn et al., 2016
Specimens observed: DPC cast holotype GSI D 107, M_2 and M_3 (both with broken paraconids); GSP-Y 26443a (Locality Y0711), M_3 fragment; GSP-Y 5884b (Y0336), maxilla with M^2, M^3 (note M^2 is reconstructed and more compact than GSP-Y 30940 M^2); GSP-Y 30940 (Y0711), maxilla with P^4, M^1, M^2; GSP-Y S-337 (S0013), M_3 fragment; GSP-Y 27923 (Y0750), canine; GSP-Y 21894 (Y0504), distal humerus; GSP-Y 10022 (Y0303), M^1 metastyle; GSP-Y 26443b (Y0711), P_4 or M_1 talonid; GSP-Y S-410 (S0002), M_2 protoconid; GSP-Y 912 (Y0048), M_3 fragment; GSP-Y 47155 (Y0758), metapodial fragment; GSP-Y 5884b, P^4; GSP-Y S-304 (S0015), P_4 talonid; GSP-Y 52181 (Y0504), distal radius; GSP-Y 36904, vertebra centrum; GSP-Y 36906 (Y0504), thoracic vertebra centrum; GSP-Y 33025 (Y0051), cervical vertebra 4^{th}?

Hyainailouros (Sivapterodon) lahirii **(Ginsburg, 1980)**
Formation:
Locality: Siwaliks
Geological Age: middle Miocene
Absolute Age: 13 Ma
Country: Pakistan
Citation: Pilgrim, 1932; Ginsburg, 1980
Specimens observed from Pilgrim, 1932: GSI D 236, dentary with M_2, M_3

Hyainailouros fourtaui
Formation:
Locality: Moghra
Geological Age: early Miocene
Absolute Age: 18–17 Ma
Country: Egypt
Citation: von Koenigswald, 1947; Savage, 1973
Specimens observed: P^4

Hyainailouros nyanzae
Formation:
Locality: Ombo (part of the Maboko sequence?), shares species with *Proconsul nyanze* from Rusinga, so may be older?
Geological Age: early Miocene
Absolute Age: 18–17 Ma
Country: Kenya
Citation: Savage, 1965
Specimens observed: NHMUK PV M holotype, P^4; "CMF 4007", P^4; "UMP 64.33", M^2

Hyainailouros napakensis **(Ginsburg, 1980)**
Formation:
Locality: Napak I, Uganda
Geological Age: early Miocene

Absolute Age: 20–19 Ma
Country: Uganda
Citation: Savage, 1965; Ginsburg, 1980
Specimens observed: Observed cast of NHMUK PV M holotype 19090 (AMNH 56436), P^4–M^2

Hyainailouros sulzeri
Formation:
Locality: Type Veltheim, Switzerland
Geological Age: MN 3–MN5
Absolute Age: 18–15 Ma
Country: France, Switzerland, Germany
Citation: Ginsburg, 1980; Morlo, Miller & El-Barkooky, 2007; Solé et al., 2015
Specimens observed: SMNS 1926 I 12, P^4–M^1 (Cast of Holotype); NHMUK PV M 14000, P^4 (Cast of specimen from Mösskirsch, Baden); NHMUK PV M 13999, M^2 (Cast of specimen from Mösskirsch, Baden); MNHN.F.Or 311-1, maxilla fragment; MNHN.F.Or 311-2, P_4 fragment, dentary with P_3–M_1 alveoli; MNHN.F.Or 311-3, distal dentary fragments; MNHN 311-4, P^4 fragment; MNHN.F.Or 311-5, P_2; MNHN.F.Or 311-6, P_2; MNHN.F.Or 311-9, M_2 protoconid; MNHN.F.Or 311-10, M_3 protoconid fragment; MNHN.F.Or 311-11, canine fragment; MNHN.F.Or 311-14, cervical vertebra; MNHN.F.Or 311-15, thoracic vertebra; MNHN.F.Or 311-16, thoracic vertebra; MNHN.F.Or 311-18, thoracic vertebra; MNHN.F.Or 311-22, lumbar vertebra; MNHN.F.Or 311-23, caudal vertebra; MNHN.F.Or 311-38, occipital condyle; MNHN.F.Or 311-39, atlas fragment; MNHN.F.Or 311-44, 45, 46, 47, 49, 50, rib fragments; MNHN.F.Or 311-51, distal humerus; MNHN.F.Or 311-52, radius; MNHN.F.Or 311-53, ulna; MNHN.F.Or 311-54, humerus; MNHN.F.Or 311-55, radius; MNHN.F.Or 311-56, ulna fragment; MNHN.F.Or 311-57, greater trochanter epiphysis; MNHN.F.Or 311-58, carpal fragment; MNHN.F.Or 311-59, cuboid; MNHN.F.Or 311-60, carpal; MNHN.F.Or 311-61, carpal; MNHN.F.Or 311-62, carpal; MNHN.F.Or 311-63, carpal; MNHN.F.Or 311-64, metatarsal; MNHN.F.Or 311-65, intermediate phalanx; MNHN.F.Or 311-66, femur; MNHN.F.Or 311-67, femoral head; MNHN.F.Or 311-68, tibia; MNHN.F.Or 311-69, fibula; MNHN.F.Or 311-70, astragalus; MNHN.F.Or 311, Calcaneum; MNHN.F.Or 311-72, calcaneal epiphysis; MNHN.F.Or 311-79, phalanx; MNHN.F.Or 311-80, phalanx; MNHN.F.Or 311-81, phalanx; MNHN.F.Or 311-82, phalanx; MNHN.F.Or 311-83, phalanx; MNHN.F.Or 311-84, phalanx; MNHN.F.Or 311-85, phalanx; MNHN.F.Or 311-86, phalanx; MNHN.F.Or 311-87, phalanx; MNHN.F.Or 311, metatarsal 2–5 and cuboid

***Hyainailouros* Arrisdrift**
Formation:
Locality: Arrisdrift
Geological Age: early middle Miocene
Absolute Age: 17–15 Ma
Country: Namibia
Citation: Morales et al., 1998; Morales et al., 2003
Specimens observed: GSN AD 100'96, dentary with M_1, erupting M_2 and M_3 (observed in Morales et al. 2003); GSN AD 375'94, M^1 (observed in Morales et al. 1998)

Indohyaenodon raoi

Formation: Cambay Shale Formation
Locality: Vastan open-cast lignite mine
Geological Age: lower Eocene, Ypresian, Bumbanian Asian Land Mammal Age
Absolute Age: 54.5 Ma
Country: India
Citation: Rose et al., 2014; Rana et al., 2015
Observed from figures in Rana et al., 2015: GU 1680, rostrum with P^2–M^3; GU 767, dentary with P_4–M_3 (canine–P_3); GU 1721, M^1 or M^2; GU 321, M_1; GU 1631, M_1; GU 652, dentary with P_4, M_2, alveoli for canine, P_2, P_3; GU 1630, dentary with alveoli for canine, P_2, P_4–M_1; GU 740, ulna; GU 741, tibia; GU 273, tibia; GU 807, calcaneus

***Isohyaenodon zadoki* (= *Isohyaenodon matthewi*, = *Metapterodon zadoki*)**
Locality: Songhor, Rusinga
Geological Age: Burdigalian, early Miocene
Absolute Age: 17–20 Ma
Country: Kenya
Citation: Savage, 1965; Morales et al., 1988; Morales and Pickford, 2017
Specimens observed: NHMUK PV M 19098 (holotype of *Isohyaenodon matthewi*), dentary with P_4, partial M_2, M_3; KNM-RU 2946, M_3; NHMUK PV M 19094 (holotype, originally, *Metapterodon zadoki*), maxilla with M^1, M^2

Isohyaenodon andrewsi
Locality: Maboko-Ombo, Rusinga, Chamtwara, Moruorot
Geological Age: Burdigalian, Langhian (early and middle Miocene)
Absolute Age: 17.5–13.6 Ma
Country: Kenya
Citation: Savage, 1965; Morales and Pickford, 2017
Specimens observed: NHMUK PV M 15048 (holotype), dentary with M_1–M_3; KNM-RU 2947, dentary with M_2, M_3; KNM-CA 2792, dentary with M_3; KNM-MO 25, dentary with P_3–M_3

Kerberos langebadrae
Formation: ?
Locality: Lautrec, Montespieu
Geological Age: MP16, middle Eocene, Bartonian
Absolute Age: 40.4–37.2 Ma
Country: France
Citation: Solé et al., 2015
Specimens observed: MNHN.F.EBA 517 (Holotype), cranium with I^2–I^3, P^1–M^3; MNHN.F.EBA 518a, dentary with canine, M_2–M_3; MNHN.F.EBA 518b, dentary with P_2–M_3; MNHN.F.EBA 520, fibula; MNHN.F.EBA 521, astragalus; MNHN.F.EBA 522, calcaneus; MNHN.F.EBA 523, metatarsal 1; MNHN.F.EBA 524, metatarsal II; MNHN.F.EBA 525, metatarsal III; MNHN.F.EBA 526, metatarsal II; MNHN.F.EBA 527, middle phalanx; MNHN.F.EBA 528, middle phalanx

Koholia atlasense
Formation: ?

Locality: El Kohol, Saharan Atlases
Geological Age: Ypresian, late early Eocene
Absolute Age: 51.8–51 Ma
Country: Algeria
Citation: Crochet, 1988; Solé et al., 2009; Coster et al., 2012
Observed from Fig. 1 and Fig. 2 in Crochet, 1988

Kyawdawia lupina
Formation: 'Upper Member' of the Pondaung Formation
Locality: Kdw7, Pondaung area
Geological Age: latest middle Eocene
Absolute Age: 40.1–36.7 Ma
Country: Myanmar
Citation: Egi et al., 2005, Zaw et al., 2014
Specimens observed as casts: AMNH 133542 (cast of holotype NMMP-KU 0042), rostrum with I^2–I^3, canine, P^1, P^4–M^3; NMMP-KU 0042 (cast at UCMP), canine cast; NMMP-KU 0784, P_4; NMMP-KU 0043, M_3; KMMP-KU 1288, I^3, canines, P_1, P_4, M_1, M_3, P^2, P^3, M^2, dentary fragments
Specimens observed from Egi et al., (2005): NMMP-KU 0042, cranium with zygomatic arch fragments; NMMP-KU 0044, I^2–I^3; NMMP-KU 1661, I^3, dentary with P_3, P_4, M_2–M_3; NMMP-KU 0785, humerus, femoral head, tibia, vertebra, jugal (all fragmentary); NMMP-KU 1288, pisiform, phalanx

Lahimia selloumi
Formation: local Thanetian bed IIa, Sidi Chennane quarries
Locality: Ouled Abdoun Basin
Geological Age: ?middle Paleocene–late Paleocene, Selandian
Absolute Age: 61.6–59.2 Ma
Country: Morocco
Citation: Solé et al., 2009; Kocsis et al., 2014
Specimens observed from casts created by E. Gheerbrant for E. Seiffert of OCP DEK/GE 443 (Holotype), dentary with alveoli for canine, P_2–P_4, M_1–M_3; MNHN.F.PM 56, dentary with M_2–M_3; MNHN.F.PM 57, dentary with P_3 roots, M_1–M_3; OCP DEK/GE 442, dentary with M_2–M_3 and alveoli of P_2–M_1

Leakitherium hiwegi
Formation: Hiwegi Formation, Kulu Formation
Locality: Rusinga Island (Kavirondo Gulf), Napak
Geological Age: Burdigalian, early Miocene
Absolute Age: 17.8–15 Ma
Country: Kenya, Uganda
Citation: Savage, 1965; Werdelin, 2010
Specimens observed: NHMUK PV M 19083 (Holotype), maxilla with M^1–M^2; KNM-RU 3119, dentary with P_4–M_3, isolated M^1, M^2, P_1– P_4, canines, cranial fragments including the sagittal crest, occipital region, and zygomatic arches; KNM-RU 2949, maxilla with dP^3, dP^4; KNM-RU

17244, astragalus; KNM-RU 4389, P^4; KNM-RU 8390, P_4; KNM-RU 17243, M_3; KNM-RU 17343, humerus; KNM-RU 15182, maxilla with dP^3, dP^4; ; KNM-RU 8369, M^2

Leonhardtina gracilis
Formation: Geiseltal
Locality: Geiseltal
Geological Age: MP12–MP13
Absolute Age: 48.6–40.4 Ma
Country: Germany
Citation: Solé et al., 2014a
Specimens observed: GMH VI-42-1949 (10237) Holotype, dentary with P_2–M_3; GMH VI-712-1951, dentary with I_1–canine, P_1 alveoli, P_2–P_4, M_2–M_3, palate with P^3–M^3, astragalus; GMH I-786-1949 (10038), cranium with P^2–M^3 and petrosal; GMH 2802, calcaneum; GMH VI-343, dentary with P_3–M_3; GMH I-78a-10038, dentary with P_3, P_4, M_3; GMH LVIII-23-1982, dentary with P_2–P_4, M_2–M_3; GMH XXXV-15-1962, maxilla with P^2–P^4

Lesmesodon behnkeae
Lesmesodon edingeri
Formation: Messel
Locality: Messel (Hessen, Germany)
Geological Age: early middle Eocene (MP 11)
Absolute Age: 48.6–40.4 Ma
Country: Germany
Citation: Morlo and Habersetzer, 1999
Specimens observed: SMF-ME 3843, skeleton with P^3, dP^4, M^1, M^2 exposed; SMF-ME 1465a, upper skeleton with canine–P_3, dP_4, M_1–M_2
Specimens also scored from observations made in Morlo and Habersetzer (1999)

Limnocyon verus
Formation: Bridger Formation
Locality: Bighorn Basin, Bridger Basin, Uinta Basin
Geological Age: Br1, Br2, Br3, middle Eocene, early to late Bridgerian
Absolute Age: 50.3–46.2 Ma
Country: USA
Citation: Ivy, 1993; Morlo and Gunnell, 2003
Specimens observed from observation: YPM 13095 (Holotype), I^1–I^3, P^1, P^4–M^2; YPM 11796, cranium with P^3–M^2; AMNH 12155, cranium with I^1–I^3 (alveoli), canine, P^1–M^2, dentary with canine–M_2, ulna, radius, humerus, femur, tibia, fibula, astragalus, calcaneum, metapodials

Maelestes gobiensis
Formation: Djadokhta Formation
Locality: Ukhaa Tolgod, Mongolia
Geological Age: Campanian, Late Cretaceous
Absolute Age: 75–71 Ma
Country: Mongolia
Citation: Wible et al., 2007; Wible et al., 2009

Specimens observed from literature in Wible et al., 2007 and Wible et al., 2009

Masrasector aegypticum
Formation: Jebel Qatrani Formation
Locality: Quarry G
Geological Age: Rupelian
Absolute Age: 31–30.6 Ma
Country: Egypt
Citation: Simons and Gingerich, 1974; Seiffert, 2010
Specimens observed: CGM 30978, dentary with P_3, M_1–M_3 (casts of holotype also observed at UCMP 66312, YPM 20943, AMNH 129736); YPM 30030, maxilla with P^3–P^4; YPM 20944, dentary with dP_4–M_1

Masrasector ligabuei
Formation: Ashawq Formation
Locality: Taqah, Dhofar Province, Sultanate of Oman
Geological Age: Priabonian, latest Eocene; Rupelian, early Oligocene
Absolute Age: 33–30.6 Ma
Country: Oman, Egypt
Citation: Crochet et al., 1990; Seiffert, 2006
Specimens observed in Crochet et al., 1990: TQ 13 (Holotype), M^1; TQ 14, M_3

Masrasector nananubis
Formation: Jebel Qatrani Formation
Locality: L-41
Geological Age: late Priabonian, latest Eocene
Absolute Age: 35–33.9 Ma
Country: Egypt
Citation: Borths and Seiffert, in press
Specimens observed: CGM 83736 (Holotype), right dentary with canine, P_2–M_3;
CGM field number 96-161, rostrum fragment with P^3–M^2; CGM field number 95-281, dentary with P_4–M_1; CGM field number 95-109, isolated M^2; DPC 7704, left dentary with P_2–M_3; DPC 8276, rostrum and palate with P^3–M^3; DPC 9274, right dentary with canine, P_1, alveoli for P_2, P_3–P_4, alveoli for M_1, $M_{2,3}$; DPC 10358, left dentary with dP_3, dP_4, $M_{1,2}$; DPC 11383, right dentary with C, alveoli for P_1, P_2–M_3; DPC 11359, right dentary with canine, P_{1-4}, M_3; DPC 11990, cranium with P^2–M^3; DPC 12157, cranium with alveoli for $P^{1,2}$, P^3–M^3; DPC 12330, right dentary with P_3–$M_{1,2}$; DPC 12524A, right dentary with alveoli for $P_{2,3}$, P_4–M_3; DPC 13285, rostral fragment with P^2–M^3; DPC 15211, left dentary with C, P_1–M_3; DPC 15742, right dentary with canine, P_2–M_3; DPC 10831, left distal humerus; DPC 15436, left distal humerus; DPC 11670, left distal humerus, DPC 13837, right maxilla dP^3, dP^4, M^1; DPC 20882, maxilla with dP^3-dP^4

Matthodon tritens
Formation: Geiseltal
Locality: Geiseltal
Geological Age: MP11

Absolute Age: 48.6–40.4 Ma
Country: Germany
Citation: Solé et al., 2014a
Specimens observed: GMH XIV-1-Franzke 6, dentary with canine, P_2–M_3, GMH XIV-739-1957, dentary with P_1–M_3; GMH XIV 5107-Franzke 9, maxilla with P^2–P^4; GMH XIU-3820, humerus; GMH XIV-2832-1956, dorsal cranium fragment

Megistotherium osteothlastes Savage 1973
Locality: Gebel Zeltan; Wadi Moghra; Bartule, Ngora Fm.
Geological Age: Burdigalian, middle Miocene
Absolute Age: 19–12 Ma
Country: Libya, Egypt, Kenya
Citation: Savage, 1973; Werdelin, 2010; Morales and Pickford, 2005
Specimens observed: NHMUK PV M 26173 (Holotype), cranium with alveoli for I^1–M^2 with partial crowns of P^2, M^2, M^3; NHMUK PV M 104574, astragalus; NHMUK PV M 26518, maxilla with alveoli for M^1–M^3; NHMUK PV M 104571, Metatarsal IV; NHMUK PV M 104572, metatarsal III; NHMUK PV M 104573, metatarsal III; NHMUK PV M 104570, distal humerus; NHMUK PV M 26516, premaxilla fragment with I^1 alveoli; NHMUK PV M 21902, atlas; NHMUK PV M 26515, cranial fragment with parietals, occipital condyles, basicranium; NHMUK PV M 92922, maxilla with roots of P^2–P^3; DPC 6611, dentary with P_4–M_3; OCO BAR 109'03, M_2

Metapterodon kaiseri
Formation: Elisabethfeld
Locality: Elisabethfeld, Rusinga Island
Geological Age: early Miocene, middle Burdigalian
Absolute Age: 20–15 Ma
Country: Namibia, Kenya
Citation: Holroyd, 1999; Werdelin, 2010
Specimens observed: BSPG 1926-X-1 (Holotype), maxilla with P^3–M^2

Metasinopa spp.
Formation: Jebel Qatrani Formation
Locality: Type locality unknown beyond "upper sequence of Jebel Qatrani"
Geological Age: Rupelian, Fayum A? (V is Where *M. osborni* comes from)
Absolute Age: 33–30 Ma
Country: Egypt
Citation: Holroyd, 1994; Lewis and Morlo, 2010; Seiffert, 2010
Specimens observed: AMNH 14453 (Holotype), dentary with canine, P_2–M_3; DPC 10199, maxilla with dP^3, dP^4, M^1; DPC 4544, dentary with P_2, dP_4, M_1, M_2, M_3.

Mlanyama sugu
Formation: Unnamed
Locality: Nakwai
Geological Age: latest Oligocene to early Miocene
Absolute Age: 24–20 Ma

Country: Kenya
Citation: Rasmussen and Gutierrez, 2009
Note: Rasmussen and Gutierrez (2009) originally described the holotype as retaining P_1–M_1 with P_4 retained as a highly modified molariform tooth. For the purposes of this study, the tooth position identified by Rasmussen and Gutierrez (2009) as P_4 is considered dP_4.
Specimens observed: KNM-NW 46832 (Holotype), dentary with canine alveolus P_2–M_1; KNM-NW 46828, P_4; KNM-NW 46824, P^4; KNM-NW 46829, P_3; KNM-NW 46830, P_3; KNM-NW 46831, M^1; KNM-NW 46909, M_3; KNM-NW 46913, M_1; KNM-NW 46914, M_3

Morlodon vellerei
Formation: ?
Locality: MP8+9, Saint Agnan (Paris Basin, France), MP8+9, Avenay, Condé-en-Brie (France)
Geological Age: Early Eocene, MP8+9, Wasatchian
Absolute Age: 55.8–48.6 Ma
Country: France
Citation: Solé, 2013
Specimens observed: StA 741-L (Holotype), dentary with P_2–M_2; StA 326, M^2 trigonid
Specimens observe from Solé, 2013: MNHN.F.Condé 65, maxilla fragment with P^4–M^3

Orienspterodon dahkoensis
Formation: Rencun Member, lower part of Heti Formation in China, Upper member of Pondaung Formation in Myanmar
Locality: Lunan Basin, Yunan Province, southern China; Eastern side of Pondaung Range, central Myanmar
Geological Age: late middle Eocene
Absolute Age: 42–39 Ma
Country: China, Myanmar
Citation: Egi et al., 2007
Specimens observed: PGM V1297, dentary with P_2–M_3; AMNH 122028 (cast of IVPP specimen), M_3; NMMP-KU 0261 (cast observed at UCMP), dentary with P_2–M_1; NMMP-KU 0262, M_1 and M_2 trigonids; NMMP-KU 0304 (cast observe at UCMP), maxilla with roots of P^3–P^4, M^1
Specimens observed in Egi et al., 2007: NMMP-KU 1628, proximal metacarpal II, metatarsal III, metatarsal IV

Oxyaenoides bicuspidens
Formation: Geiseltal
Locality: Geiseltal
Geological Age: MP11
Absolute Age: 48.6–40.4 Ma
Country: Germany
Citation: Solé et al., 2014a; Solé, 2015
Specimens observed: GMH XIV-2848-1955 (Holotype, cast also available as UCMP 140637), dentary with P_2–M_3; GMH XV-1143-1957, calcaneum; GMH XIV-2944-Franzke 9, maxilla with alveoli for P^1–P^4, crowns of M^1–M^2; GMH XIV-2909-1954, dentary with M_1–M_3; GMH XIV-

2910-Franzke 12, premaxilla fragment and maxilla fragment with M^1–M^2; GMH XIV-291, P_4; GMH XXXVII-174-1970, femur; GMH XIV-2810-1954, humerus; GMH XIV-456-1956, femur

Oxyaenoides lindgreni
Formation: Cuis, Mancy
Locality: Cuis, Mancy
Geological Age: MP10
Absolute Age: 51–48.6 Ma
Country: France
Citation: Solé et al., 2014a; Solé, 2015
Specimens observed: MNHN.F.L-49-MA (Holotype), dentary with P_4, M_2, M_3 (casts at MCZ 21254, UCMP 107092); MNHN.F.MA 14826, dentary with P_3–P_4; MNHN.F.L 23-Cuis, M^1; MNHN.F.MA 14833, M_1
Observed in Solé et al., 2014a

Paratritemnodon indicus
Formation: Subathu Formation, upper part
Locality: Outer Himalaya, near Village Fiji on the Metka-Mohgala Road, Rajauri District
Geological Age: Late Early to early Middle Eocene
Absolute Age: 49–44.5 Ma
Country: India
Citation: Kumar, 1992; Rana et al., 2015
Observed from Fig. 2 (WIF/A 1103, palate with canine–M^3) and Fig. 3 (WIF/A 1102, dentary with P_3–M_3) in Kumar (1992)

Paroxyaena galliae
Formation: Quercy
Locality: Quercy, France
Geological Age: middle Eocene, Bartonian
Absolute Age: 41.2–37.8 Ma
Country: France
Citation: Lange-Badré, 1979; Solé et al., 2015
Specimens observed: MNHM Qu 8735, dentary with P_4–M_3; BSPG 1879-XV-33, maxilla with M^1, M^2
Specimens observed observed from Lange-Badré, 1979

Paroxyaena pavlovi
Formation: Specific locality unknown
Locality: Quercy, France
Geological Age: late Eocene, Priabonian, MP16
Absolute Age: 40.4–37.2 Ma
Country: France
Citation: Lavrov, 2007; Solé et al., 2015
Observed from cast of GGM Ca-300 courtesy of A. Lavrov
Observed from literature in Figs. 1–4, GGM Ca-300, cranium with dP^3, dP^4, M^1

Parvagula palulae
Formation: ?
Locality: Palette, Provence, Bouches-du-Rhone; Fornes, Minervois, Hérau
Geological Age: Early Eocene (not more specific in Solé et al., 2015, Ypresian age used here)
Absolute Age: 56–47.8 Ma
Country: France
Citation: Godinot et al., 1987; Solé et al., 2015
Specimens observed: UM/PAT 4 (Holotype, cast observed at MNHM), dentary with P_2–M_1
Specimens observed in Solé et al., 2015: UM/FNR 52, trigonid of M_1; UM/FNR 53, dentary fragment with P_4; UM/FDN 153, trigonid of M_1

Preregidens langebadrae
Formation: Argiles rutilantes d'Issel et de Saint-Papoul Formation
Locality: Saint-Papoul, Aude, Languedoc-Roussillon
Geological Age: early Eocene, Ypresian, MP8 and MP9
Absolute Age: 55.8–48.6 Ma
Country: France
Citation: Solé et al., 2015
Specimens observed in Solé et al. (2015): MNHN.F.SPPXX1, dentary with P_1, P_2, P_3 alveoli, P_4, M_1– M_3

Prolimnocyon atavus
Formation: Willwood Formation
Locality: Clark's Fork Basin, Bighorn Basin, Powder River Basin, Piceance Creek Basin, San Juan Basin, Washakie Basin
Geological Age: early Eocene, Wasatchian, Wa3 to Wa6
Absolute Age: 53–50 Ma
Country: USA
Citation: Gebo and Rose, 1993; Gunnell, 1998
Specimens observed: DPC 5364, maxilla with P^4–M^3, dentary with P_1–M_3, scapula fragment, humerus, radius, ulna, ungula phalanx, innominate, femur, tibia, fibula fragment, calcaneum, astragalus, cuboid, metatarsals, vertebrae
Also referenced illustrations in Gebo and Rose (1993)

Prolimnocyon chowi
Formation: Nomogen Formation
Locality: Bayan Ulan, Inner Mongolia
Geological Age: late Paleocene
Absolute Age: 57–55.3 Ma
Country: China
Citation: Meng et al., 1998
Specimens observed from figures in Meng et al. (1998)

Propterodon morrisi
Formation: Irdin Manha Beds, Iren Dabasu Basin
Locality: "23 miles south of Iren Dabasu"

Geological Age: middle middle Eocene, Irdinmanhan Age
Absolute Age: 46–43 Ma
Country: Mongolia
Citation: Matthew and Granger, 1924
Specimens observed: 19160 (Holotype), dentary with P_2, dP_4, M_2; AMNH 21553, dentary with P_2, M_1–M_3; AMNH 95776, dentary with canine, P_2–M_2; AMNH 96384, dentary with P_2, roots of P_3, P_4–M_2; AMNH 95777, dentary with P_2–M_3 PIN 71-73, P_3, M_2, M_3 trigonid, dP_4, M^2

Propterodon tongi
Formation: Hedi Formation, Yuli member
Locality:Huoshipo, Guojia Village, Wangmao Town, Yuanqu, Shanxi
Geological Age: middle middle Eocene, Irdinmanhan Age
Absolute Age: 46–43 Ma
Country: China
Citation: Liu et al., 2002
Specimens observed: IVPP V12612 (Holotype), dentary with P_1–M_3

Prototomus minimus
Formation: Tienen Formation
Locality: Dormaal
Geological Age: MP7
Absolute Age: 55.8–48.6 Ma
Country: Belgium
Citation: Smith and Smith, 2001
Specimens observed: IRSNB M1287 (Holotype), M_1; IRSNB M 1286, P_4; IRSNB M 1288, M_2; IRSNB M 1289, M_3; IRSNB M 1290, P_4; IRSNB M 1291, M^1; IRSNB M 1292, M^2; IRSNB M 1293, M^3; IRSNB M 1294, edentulous dentary; IRSNB M 1295, edentulous dentary; IRSNB M 1285, dP_4

Prototomus phobos
Formation: Many (Willwood Formation, Bridger Formation etc.)
Locality: Clarks Fork Basin, Bighorn Basin, Powder River Basin
Geological Age: Early to Middle Eocene, earliest Wasatchian Wa0 to earliest Bridgerian BR0
Absolute Age: 55–46 Ma
Country: USA, Europe
Citation: Gingerich and Deutsch, 1989; Ivy, 1993; Zack, 2011; Solé et al., 2014a
Specimens observed: YPM-PU 13019 (Holotype), cranium with I^1–I^2, P^1–P^2, P^4–M^3 and dentaries with C–M_3; UM 68075, dentary with C, P_3, and portions of M_1–M_3; UM 74134, maxilla with M^1–M^3, astragalus, calcaneum, humerus

Proviverra typica
Formation: Geiseltal level XXXVI
Locality: Geiseltal, Germany
Geological Age: Geiseltalian, Lutetian, Middle Eocene
Absolute Age: 46–41 Ma
Country: Germany

Citation: Solé et al., 2014a
Specimens observed: NMB Em 18 (Holotype), cranium with alveoli of canine, roots of P^1, P^4, M^1, M^2 (protocone), M^3; NMB Ek 30 (cast also viewed: UCMP 140643), maxilla with P^4–M^3; NMB Eh 561 (cast also viewed: UCMP 140642), dentary with P_4, M_2–M_3; GMH XXXVI-519 (cast also viewed: UCMP 140641), dentary with P_4–M_2; GMH XXXVII-136-1964, dentary with P_2–P_3, fragments of P_4, M_1, fragments of M_2–M_3; GMH XXXVI-20-1962, dentary with P_3–P_4, M_2 (talonid)–M_3; GMH XLI-309-1968, dentary with P_4–M_1; NMB 162, maxilla with P^4–M^2; NMB Eh. 191, P_3, M_1–M_3

"*Pterodon*" *africanus* Andrews 1903
Formation: Jebel Qatrani Formation
Locality: Quarry A, lower sequence, Fayum Depression
Geological Age: early Oligocene
Absolute Age: 33.9–33.7 Ma
Country: Egypt
Citation: Holroyd, 1994; Holroyd, 1999; Seiffert, 2010
Specimens observed: BSPG 1905-XIII-8 (Holotype), dentary with canine–M_3; AMNH 13251, maxilla with P^2–P^3, fragmentary P^4–M^2; CGM 8897 (cast at NHMUK PV M 8887), femur; CGM 8898, humerus; UCMP 41475, maxilla with M^2; SMNS 43470, calcaneum; SMNS 11575, cranium with incisor alveoli, canine, P^2–M^3, posterior portion of cranium very heavily reconstructed; SMNS 43471, tibia; NHMUK PV M 8503, dentary with P_2–M_3; NHMUK PV M 21897, palate with P^2–M^2; NHMUK PV M 8445, proximal femur; NHMUK PV M 9475, astragalus; NHMUK PV M 9473, axis fragment; NHMUK PV M 9472, axis; NHMUK PV M 9472, atlas; NHMUK PV M 9472, cervical vertebra; NHMUK PV M 8446, vertebra

Pterodon dasyuroides de Blainville 1839
Formation: Quercy
Locality: Paris Basin
Geological Age: MP18–MP20, Priabonian, Late Eocene
Absolute Age: 37.2–33.9 Ma
Country: Paris
Citation: Lange-Badré, 1979; Solé et al., 2014a; Solé et al. 2015
Specimens observed: MNHM 1903-20.Qu.8652 (Holotype), cranium with Canine–M^3; MNHM 1893-11.Qu 8301, dentary with I_3, P_1–M_3 and cranium with I^2, canine, P^2–M^3;MNHM 1893-11.Qu 8304, cranium with P^2–M^3; MNHM 1882-18.Qu 8803, dentary with P_4–M_3; MNHM 1903-80.Qu 8669, rostrum with I^1–I^2, canine, P^2–M^3; MNHM 1903-20.Qu 8631, basicranium; MNHM 1893-11.Qu 8736, dentary with canines, P_2 –M_3; MNHM Qu 8734, maxilla with canine–M^3; MNHM 1875-931.Qu 8787, maxilla with P^3–M^3; MNHM 1903-20.Qu 10071, calcaneum; MCZ 8912, dentary with P_2–M_3; MCZ 8911, maxilla with P^3–M^2; BSPG 1879 1879-XV-32, maxilla with P^4–M^3; BSPG 1961-XVII-19, maxilla fragment with M^2; BSPG 1959-IX-4, maxilla with M^1–M^2; NHMUK PV M 27578, maxilla with P^2, P^4, M^1–M^2; NHMUK PV M 26757, maxilla with P^4–M^3; BSPG 1879 XV 642, dP^3

"*Pterodon*" *phiomensis* Osborn 1909
Formation: Jebel Qatrani Formation
Locality: Quarry A, Fayum Depression

Geological Age: early Oligocene
Absolute Age: 33.9–33.7 Ma
Country: Egypt
Citation: Holroyd, 1994; Holroyd, 1999; Seiffert, 2010
Specimens observed: AMNH 13253 (Holotype), P_2–M_3; AMNH 13254, dentary with P_2–M_3

Pyrocyon strenuus Gingerich and Deutsch 1989
Formation: San Jose Formation
Locality: San Jose Basin, Bighorn Basin, Wind River, Green River
Geological Age: Early to Middle Eocene, middle Wasatchian (Graybullian) Wa3 through Bridgerian (Br1) (*P. multicuspis* is early Eocene, middle to late Wasatchian (late Graybullian Wa5) to Lostcabinian (Wa7)
Absolute Age: 55.8–50.3 Ma
Country: USA
Citation: Ivy, 1993; Gingerich and Deutsch, 1989
Specimens observed: USNM 1023 (Holotype), dentary with canine, P_2–M_3; AMNH 15234, maxilla with canine–M^3 and dentary with canine–M_3; UM 21186, dentary with P_2, P_4–M_3

Quasiapterodon minutus
Formation: Jebel Qatrani Formation, Quarry M
Locality: Fayum Depression
Geological Age: Rupelian, Younger than G and V (in turn older than A and B)
Absolute Age: 30–29.2 Ma
Country: Egypt
Citation: Lavrov, 1999; Grohé et al., 2012
Specimens observed: SMNS with no number (Holotype, cast of type also available at UCMP 140656), dentary with part of P_4, M_1–M_3; DPC 2948, maxilla with P^3–M^3; DPC 8288, maxilla with P^4–M^1; DPC 7314, maxilla with P^3–M^1; DPC 21473, dentary with P_4–M_3; DPC 3154, dentary with canine, P_2–M_3; DPC 201431, dentary with canine, P_3–M_3; DPC 5022, dentary with M_1–M_2; DPC 2949, dentary with P_4–M_3;

Quercytherium simplicidens
Formation: Quercy phosphorites
Locality: Quercy phosphorites
Geological Age: early late Eocene
Absolute Age: 37.2–33.9 Ma
Country: France
Citation: Lange-Badré, 1979; Solé, et al., 2014a
Specimens observed: MNHN unnumbered right dentary with P_2–M_3; MNHN.F.Qu 8559, dentary with P_4, portions of M_1–M_3; MNHN.F.Qu 1962-35, dentary with M_2–M_3; MNHN.F.Qu 1893-11, left dentary with P_2–P_4, M_3; MNHN.F.Qu 8645, dentary with M_2–M_3; MNHN.F.Qu 8649, cranium with P^2, P^4, M^2, M^3

Quercytherium tenebrosum
Formation: See localities
Locality: Euzet-les-Bains (Gard), Quercy phosphorites
Geological Age: early late Eocene

Absolute Age: 40–33.9 Ma
Country: France
Citation: Lange-Badré, 1979; Solé, et al., 2014
Specimens observed: MNHN.F.Qu 8644 (Holotype), dentary with P_2–M_3; MNHN.F.Qu 8643, dentary with P_2–M_3; MNHN.F.Qu 8646, maxilla with P^1–M^3

Sectisodon markgrafi
Locality: unknown Fayum quarry, but likely Quarry A or B
Geological Age: Rupelian, Oligocene
Absolute Age: 33.9–33.7 Ma
Country: Egypt
Citation: Holroyd, 1999; Morales and Pickford, 2017
Specimens observed: AMNH 14452, maxilla with P^2–M^2

Simbakubwa kutokaafrika
Locality: Meswa Bridge
Geological Age: earliest Miocene
Absolute Age: 22–23 Ma
Country: Kenya
Citation: This study and Harrison and Andrews, 2009
Specimens observed: KNM-ME 20A (holotype), canine, P_4, M_3; KNM-ME 12, canine; KNM-ME 23, M_1; KNM-ME 22, M_2; KNM-ME 20AI, M^2; KNM-ME 20B, Canine, P^4, M^1, M^2; KNM-ME 20P, calcaneum

Sinopa grangeri
Formation: lower Bridger (B3?) Formation
Locality: Uinta County, Wyoming, Bridger Basin, Uinta Basin
Geological Age: Middle Eocene, Early to late Bridgerian (Br1 to Br3)
Absolute Age: 50.3–46.2 Ma
Country: USA
Citation: Matthew, 1906; Ivy, 1993
Specimens observed: USNM 5341 (Holotype), cranium with Canine–P^2, P^4–M^3, dentaries with canines–M_3, cervical, thoracic, lumbar, caudal vertebral series, scapula, humerus, ulna, radius, carpals, metacarpals, innominate, femur, tibia, fibula, astragalus, calcaneum, metatarsals (mounted at USNM making it difficult to observe morphology so observations were supplemented by figures in Matthew, 1906)

Sinopa jilinia
Formation: Member III, Huadian Formation
Locality: Huadian basin, Huadian County, Jilin Province
Geological Age: middle Eocene, Yuanquan (Uintan)
Absolute Age: 46.2–40.4 Ma
Country: China
Citation: Morlo et al., 2014
Specimen observed from Morlo et al. (2014): RCPS-CAMHD06-001, dentary with P_2–P_3, roots of P_4, M_1–M_3 (cast available at SMF)

Teratodon spekei
Teratodon enigmae
Formation: ?
Locality: Koru, Songhor (*T. enigmae* from Songhor only), and Rusinga
Geological Age: Burdigalian, Early Miocene
Absolute Age: 20–15 Ma
Country: Kenya
Citation: Savage, 1965; Werdelin, 2010
Specimens observed: AMNH 56429 (cast of *T. enigmae* holotype NHMUK PV M 19089, cast also available as UCMP 77538), dentary with roots of P_2–P_4, alveoli of M_1–M_3; AMNH 56428 (cast of *T. enigmae* holotype, cast also at UCMP 77535), maxilla with P^2–M^3; AMNH 56425 (original BNMH M14310, cast of *T. spekei* holotype), maxilla with canine, P^2; AMNH 56427 (cast of *T. spekei* paratype, also UCMP 77543), dentary with P^2–P^3; AMNH 56426 (cast of NHMUK PV M 14216, also available at UCMP 77541), dentary with M_2–M_3; AMNH 56424 (cast of *T. spekei* holotype NHMUK PV M 14307, also available at UCMP 77542), maxilla with P^4–M^2; UCMP 77544 (cast of NHMUK PV M 14308), dentary with P_2–P_3; KNM-SO 85, M_2; KNM-SO 1110, dentary with P_2–P_3, M_1–M_3; KNM-SO 1109, dentary with M_1–M_3; KNM-SO 1111, mandibular condyles, P_1–P_2; KNM-SO 5118, P^4; KNM-CA 311, P_3; KNM-CA 1915, dentary with P_3–P_4; KNM-RU 14769, maxilla with canine–P^4, dentary with P_2–P_4, roots of M_1–M_3; KNM-ME 29, dentary with P_2–M_2; KNM-LG 679, maxilla with P^4–M^2

Thinocyon velox
Formation: Grizzly Buttes, Blacks Fork Member, Bridger Formation (Type)
Locality: Bridgerian biochrons Br-1b, Br-2 northern and southern Green River Basin, Br-3 Washakie Basin, Wyoming
Geological Age: middle Eocene, Br1–Br3
Absolute Age: 50.3–46.2 Ma
Country: USA
Citation: Morlo and Gunnell, 2003
Specimens observed: YPM 11797, dentary with canine, P_1, fragmentary P_2–P_3, P_4, partial M_1–M_2; AMNH 13081, cranium with P^1–M^2, dentary with P_2–M_2, ulna, radius, metacarpals, sacrum; AMNH 140007, cranium and dentary (occluded) with I^1–M^2 and I_1–M_2; AMNH 11524, femur, tibia; AMNH 12154, atlas, axis, cervical, thoracic, and lumbar vertebrae, humerus, radius, ulna, carpals, femur, tibia, metapodials, astragalus, calcaneum
Specimens observed rom Morlo and Gunnell (2003): GMUW 3059, humerus, astragalus, calcaneum

Tinerhodon disputatum
Formation: Adrar Mgorn 1 and Ihadjamene
Locality: Ouarzazate Basin
Geological Age: Thanetian, Late Paleocene
Absolute Age: 56.5–55.8 Ma
Country: Morocco
Citation: Gheerbrant, et al., 2006; Seiffert, 2010

Specimens from literature (Gheerbrant et al., 2006): THR 192 (Holotype), M_3; THR 294, P_2; THR 292, P_4; THR 193, M_2; THR 192, M_3; THR 313, P_3; IDJ 1, M_1 or M_2; THR 111, M_1 or M_2

Tritemnodon agilis
Formation: Bridger Formation
Locality: Type from Grizzly Buttes, Uinta County; Bighorn basin, Bridger basin, Uinta basin
Geological Age: middle Eocene, early to middle Bridgerian (Br1 to Br2)
Absolute Age: 50.3–46.2 Ma
Country: USA
Citation: Matthew, 1909; Ivy, 1993
Specimens observed: AMNH 11536, calcaneum, astragalus, femur, tibia, fibula, atlas, innominate, sacrum, vertebrae, metapodials, metatrasals, phalanges, maxilla with canines–M^3, dentaries with canines–M_3; AMNH 12636, cranium with canines–M^3; dentaries with canine–M_3; complete cervical, thoracic, lumbar and partial caudal vertebral series, scapulae, humerus, ulna, radius, metapodials, carpals, phalanges, innominate, femur, tibia, fibula, metatarsals, astragalus, calcaneum, metapodials, phalanges

LITERATURE CITED

Bastl, K., Nagel, D., and Peigné, S. 2014. Milk tooth morphology of small-sized *Hyaenodon* (Hyaenodontidae, Mammalia) from the European Oligocene—evidence of a *Hyaenodon* lineage in Europe. *Palaeontographica, Abt A: Palaeozoology–Stratigraphy*, 303:61-84. doi: 10.1127/pala/303/2014/61

Barry, J. C. 1988. *Dissopsalis*, a middle and late Miocene proviverrine creodont (Mammalia) from Pakistan and Kenya. Journal of Vertebrate Paleontology 8:25–45.

Beck, R. M. D., and M. S. Y. Lee. 2014. Ancient dates or accelerated rates? Morphological clocks and the antiquity of placental mammals. Proceedings of the Royal Society B 281:20141278.

Becker, D., G. Rauber, and L. Scherler. 2013. New small mammal fauna of late Middle Eocene age from a fissure filling at La Verrerie de Roches (Jura, NW Switzerland). Revue de Paléobiologie, Genéve 32:433–446.

Borths, M.R., and N. J. Stevens. 2017. Taxonomic affinities of the enigmatic *Prionogale breviceps*, early Miocene, Kenya. Historical Biology https://doi.org/10.1080/08912963.2017.1393075.

Coster, P., M. Benammi, M. Hahboubi, R. Tabuce, M. Adaci, L. Marivaux, M. Bensalah, S. Mahboubi, A. Mahboubi, F. Mebrouk, C. Maameri, and J-. J. Jaeger. 2012. Chronology of the Eocene continental deposits of Africa: Megnetostratigraphy and biostratigraphy of the El Kohol and Glib Zegdou Formations, Algeria. Geological Society of America Bulletin 124:1590–1606. doi: 10.1130/B30565.1

Chang, S., H. Zhang, P. R. Renne, and Y. Fang. 2009. High-precision $^{40}Ar/^{39}Ar$ age for the Jehol Biota. Palaeogeography, Palaeoclimatology, Palzeoecology 280:94–104. doi:10.1016/j.palaeo.2009.06.021

Crochet, J. -Y. 1988. Le plus ancien créodonte africain: *Koholia atlasense* nov. gen., nov. sp. (Eocène inférieur d'El Kohol, Atlas saharien, Algérie). Comptes Rendus de l'Académie des Sciences, Paris, Série II 307:1795–1798.

Crochet, J. -Y., H. Thomas, J. Roger, and S. Al-Sulaimani. 1990. Première découverte d'un créodonte dans la péninsule Arabique: *Masrasector ligabuei* nov. sp. (Oligocène inférieur de Taqah, Formation d'Ashawq, Sultanat d'Oman). Comptes rendus de l'Académie des sciences, Paris, Série II 311:1455–1460.

Egi, N., T. Tsubamoto, and M. Takai. 2007. Systematic status of Asian "*Pterodon*" and early evolution of hyaenaelurine hyaenodontid creodonts. Journal of Paleontology 81:770–778.

Egi, N., P. A. Holroyd, T. Tsubamoto, A. N. Soe, M. Takai, R. L. Ciochon. 2005. Proviverrine hyaenodontids (Creodonta: Mammalia) from the Eocene of Myanmar and a phylogenetic analysis of the proviverrines from the para-Tethys area. Journal of Systematic Palaeontology 3:337–358.

Flynn, L. J., D. Pilbeam, J. C. Barry, M. E. Morgan, and S. M. Raza. 2016. "Siwalik Synopsis: A long stratigraphic sequence for the later Cenozoic of South Asia." Comptes Rendus Palevol. 15(7):877–887.

Fox, R. C. 2015. A revision of the Late Cretaceous-Paleocene eutherian mammal *Cimolestes* Marsh, 1889. Canadian Journal of Earth Sciences 52:1137–1149. dx.doi.org/10.1139/cjes-2015-0113

Gebo, D., and K. Rose. 1993. Skeletal morphology and locomotor adaptation in *Prolimnocyon atavus,* an Early Eocene hyaenodontid creodont. Journal of Vertebrate Paleontology 13:125–144.

Gheerbrant, E., M. Iarochene, M. Amaghzaz, and B. Bouya. 2006. Early African hyaenodontid mammals and their bearing on the origin of Creodonta. Geological Magazine 143(4): 475–489.

Gingerich, P. D., and H. A. Deutsch. 1989. Systematics and evolution of early Eocene Hyaenodontidae (Mammalia, Creodonta) in the Clarks Fork Basin, Wyoming. Contributions from the Museum of Paleontology 27:327–391.

Godinot, M. 1981. Les mammiféres de Rians (Éocéne inférieur, Provence). Palaeovertebrata 10:43–126.

Godinot, M., J. Y. Crochet, J. L. Hartenberger, B. Lange-Badré, D. E. Russell, and B. Sigé. 1987. Nouvelles données sur les mammifères de Palette (Eocène inférieur, Provence). Münchner Geowissenschaftliche Abhandlungen A10:273–288.

Grohé, C., M. Morlo, Y. Chaimanee, C. Blondel, P. Coster, X. Valentin, M. Salem, A. A. Bilal, J. -J. Jaeger, and M. Brunet. 2012. New Apterodontinae (Hyaenodontida) from the Eocene locality of Dur At-Talah (Libya): systematic, paleoecological, and phylogenetical implications. PLOS ONE 7(11):e49054.

Gunnell, G. F. 1998. Creodonta; pp. 91–109 in C. M. Janis, K. M. Scott and L. L. Jacobs (eds.), Evolution of the Tertiary Mammals of North America. Volume 1: Terrestrial carnivores, ungulates, and ungulate like mammals. Cambridge University Press, Cambridge.

Hartenberger, J.-L. 1970. Les mammiferes d'Egerkingen et l'histoire des faunes de l'Eocene d'Europe. Comptes Rendus de la Societe geologique de France 12:886-893.

Holroyd, P. A. 1994. An examination of dispersal origins of Fayum Mammalia. Ph.D. dissertation, Duke University, Durham, 328 pp.

Holroyd, P. A. 1999. New Pterodontinae (Creodonta: Hyaenodontidae) from the late Eocene–early Oligocene Jebel Qatrani Formation, Fayum province, Egypt. PaleoBios 19(2):1–18.

Huang, X.-S., and B.-C. Zhu. 2002. Creodont (Mammalia) remains from the early Oligocene of Uiantatal, Nei Mongol. Vertebrata PalAsiatica 40:21–30.

Ivy, L. 1993. Systematic revision of early to middle Eocene North American Hyaenodontidae (Mammalia, Creodonta). Ph.D. dissertation, University of Colorado at Boulder, 463 pp.

Kielan-Jaworowska, Z., R. L. Cifelli, and Z. -X. Luo. 2004. Mammals from the Age of Dinosaurs. Columbia University Press, New York, 630 pp.

Kocsis, L., E. Gheerbrant, M. Mouflih, H. Capetta, J. Yans, and M. Amaghzaz. 2014. Comprehensive stable isotope investigation of marine biogenic apatite from the late Cretaceous–early Eocene phosphate series of Morocco. Palaeogeography, Palaeoclimatology, Palaeoecology 394:74–78.

Kumar, K. 1992. *Paratritemnodon indicus* (Creodonta: Mammalia) from the early Middle Eocene Subathu Formation, NW Himalaya, India, and the Kalakot mammalian community structure. Paleontologische Zeitschrift 66:387–403.

Lange-Badré, B. 1979. Les créodontes (Mammalia) d'Europe occidentale de l'Éocène supérieur à l'Oligocène supérieur. Mémoires du Muséum National d'Histoire Naturelle 42:1–249.

Lange-Badré, B. 1984. *Hurzelerius torvidus* (Van Valen), nouveau genre de Créodontes (Mammalia) du Bartonien inférieur d'Egerkingen (Suisse) en replacement de *Prototomus*

torvidus Van Valen. Comptes Rendus de l'Académie des Sciences, Paris, Série II 299:739-742.

Lange-Badré, B., and M. Böhme. 2005. *Apterodon intermedius*, sp. nov., a new European creodont mammal from MP22 of Espenhain (Germany). Annals de Paléontologie 91:311–328.

Lavrov, A. V. 1996. A new genus *Neoparapterodon* (Creodonta, Hyaenodontidae) from the Khaichin-Ula-2 locality (Khaichin Formation, Middle-Upper Eocene, Mongolia) and the systematic position of the Asiatic *Pterodon* representatives. Paleontological Journal 30:593–604.

Lavrov, A. V. 1999. New material on the Hyaenodontidae (Mammalia, Creodonta) from the Ergiligyn Dzo Formation (Late Eocene of Mongolia) and some notes on the system of the Hyaenodontidae. Paleontological Journal 33:321–329.

Lavrov, A. V. 2007. A new species of *Paroxyaena* (Hyaenodontidae, Creodonta) from Phosphorites of Quercy, Late Eocene, France. Paleontological Journal 41:298–311.

Lewis, M. E., and M. Morlo. 2010. Creodonta; pp. 543–560 in L. Werdelin and W. Sanders (eds.), Cenozoic Mammals of Africa. University of California Press, Berkeley.

Lillegraven, J. A. 1969. Latest Cretaceous mammals of upper part of the Edmonton Formation of Alberta, Canada, and review of marsupial–placental dichotomy in mammalian evolution. Paleontological Contribution of the University of Kansas 50:1–122.

Liu, L.-P., and X.-S. Huang. 2002. *Propterodon* (Hyaenodontidae, Creodonta, Mammalia) from the middle Eocene of Yuanqu Basin, Shanxi Province. Vertebrata PalAsiatica 40:133–138.

Matthew, W. D. 1901. Additional observations on Creodonta. Bulletin of the American Museum of Natural History 14:1–38.

Matthew, W. D. 1906. The osteology of *Sinopa,* a creodont mammal of the middle Eocene. Proceedings of the United States National Museum 30:203–233.

Matthew, W. D. 1909. The Carnivora and Insectivora of the Bridger Basin, middle Eocene. Memoirs of the American Museum of Natural History 9:289–567.

Matthew, W. D. 1915. A revision of the lower Eocene Wasatch and Wind River faunas, Part 1, Order Ferae (Carnivora), suborder Creodonta. Bulletin of the American Museum of Natural History 34:4–103.

Matthew, W. D., and W. Granger. 1924. New Carnivora from the Tertiary of Mongolia. American Museum Novitates 104:1–9.

Mellett, J. S. 1969. A skull of *Hemipsalodon* (Mammalia, Deltatheridia) from the Clarno Formation of Oregon. American Museum Novitates 387:1–19.

Mellett, J. S. 1977. Paleobiology of North American *Hyaenodon* (Mammalia, Creodonta). Contributions to Vertebrate Evolution 1:1–134.

Meng, J., R. Zhai, and A. R. Wyss. 1998. The late Paleocene Bayan Ulan fauna of inner Mongolia, China; pp. 148–185 in K. C. Beard, M. R. Dawson (eds.), Dawn of the age of mammals in Asia. Bulletin of Carnegie Museum of Natural History, Pittsburgh.

Moore, J. R., G. P. Wilson, M. Sharma, H. R. Hallock, D. R. Braman, and P. R. Renne. 2014. Assessing the relationships of the Hell Creek–Fort Union contact, Cretaceous–Paleogene boundary, and Chicxulub impact ejecta horizon at the Hell Creek Formation lectostratotype, Montana, USA. Geological Society of America Special Papers 503:123–135. Doi:10.1130/2014.2503(04)

Morales, J., and M. Pickford. 2017. New hyaenodonts (Ferae, Mammalia) from the early Miocene of Napak (Uganda), Koru (Kenya) and Grillental (Namibia). Fossil Imprint 73:332–359.

Morales, J., M. Pickford, and D. Soria. 1998. New carnivores from the basal middle Miocene of Arrisdrift, Namibia. *Eclogae Geologicae Helvetiae* 91:27–40. http://doi.org/10.5169/seals-168406

Morales, J., M. Pickford, S. Fraile, M.J. Salesa, and D. Soria. 2003. Creodonta and Carnivora from Arrisdrift, early middle Miocene of southern Namibia. *Memoir of the Geological Survey of Namibia* 19:177–194.

Morales J, Pickford M, Salesa M. 2008. Creodonta and Carnivora from the early Miocene of the northern Sperrgebiet, Namibia. Mem Geol Surv Namibia. 20:291–310.

Morlo, M., and G. F. Gunnell. 2003. Small limnocyonines (Hyaenodontidae, Mammalia) from the Bidgerian middle Eocene of Wyoming: *Thinocyon, Prolimnocyon,* and *Iridodon,* new genus. Contributions from the Museum of Paleontology, The University of Michigan 31:43–78.

Morlo, M., and J. Habersetzer. 1999. The Hyaenodontidae (Creodonta, Mammalia) from the lower Middle Eocene (MP 11) of Messel (Germany) with special remarks on new x-ray methods. Courier Forschungsinstitut Senckenberg 216:31–73.

Morlo, M., and D. Nagel. 2006. New remains of Hyaenodontidae (Creodonta, Mammalia) from the Oligocene of Central Mongolia. Annals de Paléontologie 92:305–321.

Morlo, M., K. Bastl, W. Wenhao, and S. F. K. Schaal. 2014. The first species of *Sinopa* (Hyaenodontida, Mammalia) from outside of North America: implications for the history of the genus in the Eocene of Asia and North America. Palaeontology 57:111–125.

Polly, P. D. 1996. The skeleton of *Gazinocyon vulpeculus* gen. et comb. nov. and the cladistic relationships of Hyaenodontidae (Eutheria, Mammalia). Journal of Vertebrate Paleontology 16:303–319.

Polly, P. D., and B. Lange-Badré. 1993. A new genus *Eurotherium* (Mammalia, Creodonta) in reference to taxonomic problems with some Eocene hyaenodontids from Eurasia. Comptes Rendus de l'Académie des Sciences, Paris, Série II 317:991–996.

Rana, R., K. Kumar, S. Zack, F. Solé, K. Rose, P. Missiaen, L. Singh, A. Sahni, and T. Smith. 2015. Craniodental and postcranial morphology of *Indohyaenodon raoi* from the early Eocene of India, and its implications for ecology, phylogeny, and biogeography of hyaenodontid mammals. Journal of Vertebrate Paleontology DOI: 10.1080/02724634.2015.965308.

Rodrigues, H. G., L. Marivaux, and M. Vianey-Liaud. 2014. Rodent paleocommunities from the Oligocene of Uiantatal (Inner Mongolia, China). PalaeoVertebrate 38:1–11.

Rose, K. D., L. T. Holbrook, R. S. Rana, K. Kumar, K. E. Jones, H. E. Ahrens, P. Missiaen, A. Sahni, and T. Smith. 2014. Early Eocene fossils suggest that the mammalian order Perissodactyla originated in India. Nature Communications 5:5570. doi:10.1038/ncomms6570

Schmidt-Kittler N, Heizmann PJ. 1991. *Prionogale breviceps* n. gen. n. sp.: evidence of an unknown major clade of eutherians in the lower Miocene of East Africa. Münch Geowiss Abh A Geol Paläontol. 19:5–16.

Savage, R. J. G. 1965. Fossil mammals of Africa: 19. The Miocene Carnivora of East Africa. Bulletin of the British Museum of Natural History (Geology) 10:239–316.

Savage, R. J. G. 1973. *Megistotherium,* gigantic hyaenodont from Miocene of Gebel Zelten, Libya. Bulletin of the British Museum of Natural History (Geology) 22:483–511.

Seiffert, E. R. 2006. Revised age estimates for the later Paleogene mammal faunas of Egypt and Oman. Proceedings of the National Academy of Sciences, U.S.A. 103:5000–5005.

Seiffert, E. R. 2010. Chronology of Paleogene mammal localities; pp. 19–26 in L. Werdelin and W. Sanders (eds.), Cenozoic Mammals of Africa. University of California Press, Berkeley.

Simons, E. L., and P. D. Gingerich. 1974. New carnivorous mammals from the Oligocene of Egypt. Annals of the Geological Survey of Egypt 4:157–166.

Smith, T., and R. Smith. 2001. The creodonts (Mammalia, Ferae) from the Paleocene–Eocene transition in Belgium (Tienen Formation, MP7). Belgian Journal of Zoology 131:117–135.

Solé, F., E. Gheerbrant, A. Mbarek, and B. Bouya. 2009. Further evidence of the African antiquity of hyaenodontid ("Creodonta", Mammalia) evolution. Zoological Journal of the Linnean Society 156:827–846.

Solé, F. 2013. New proviverrine genus from the early Eocene of Europe and the first phylogeny of late Palaeocene–middle Eocene hyaenodontidans (Mammalia). Journal of Systematic Palaeontology 11:375–398.

Solé, F. 2015. New fossils of Hyaenodonta (Mammalia, Placentalia) from the Ypresian an Lutetian of France, and their bearing on the evolution of the Proviverrinae in Southern Europe. Paleontology.

Solé, F., J. Falconnet, and L. Yves. 2014a. New proviverrines (Hyaenodontida) from the early Eocene of Europe; phylogeny and ecological evolution of the Proviverrinae. Zoological Journal of the Linnean Society 171:878–917.

Solé, F., T. Smith, R. Tabuce, and B. Marandat. 2015. New dental elements of the oldest proviverrine mammal, *Parvagula palulae*, from the early Eocene of Southern France support possible African origin of the subfamily. Acta Palaeontologica Polonica doi:http://dx.doi.org/10.4202/app.00146.2014.

Solé, F., J. Lhuillier, M. Adaci, M. Bensalah, M. Mahboubi, and R. Tabuce. 2014b. The hyaenodontidans from the Gour Lazib area (?early Eocene, Algeria): implications concerning the systematics and the origin of the Hyainailourinae and Teratodontinae. Journal of Systematic Paleontology 12:303–322.

Solé, F., Amson, E., Borths, M., Vidalenc, D., Morlo, M., and Bastl, K. 2015. A new large hyainailourine from the Bartonian of Europe and its bearings on the evolution and ecology of massive hyaenodonts (Mammalia). PLOS ONE 10(10):e0141941. doi: 10.1371/journal.pone.0141941

Vislobokova, I. A. 2008. The oldest representative of Entelodontoidea (Artiodactyla, Suiformes) from the Middle Eocene of Khaichin Ula II, Mongolia, and some evolutionary features of this superfamily. Paleontological Journal 42:643–654.

Werdelin, L. 2010. Chronology of Neogene Mammal Localities; pp. 27–43 in L. Werdelin and W. Sanders (eds.), Cenozoic Mammals of Africa. University of California Press, Berkeley.

Wible, J. R., G. W. Rougier, M. J. Novacek, and R. J. Asher. 2007. Cretaceous eutherians and Laurasian origin for placental mammals near the K/T boundary. Nature 447:1003–1006.

Wible, J. R., G. W. Rougier, M. J. Novacek, and R. J. Asher. 2009. The eutherian mammal *Maelestes gobiensis* from the late Cretaceous of Mongolia and the phylogeny of Cretaceous Eutheria. Bulletin of the American Museum of Natural History 327:1–123.

Zack, S. P. 2011. New species of the rare early Eocene creodont *Galecyon* and the radiation of the early Hyaenodontidae. Journal of Paleontology 85:315–336.

Zaw, K., S. Meffre, M. Takai, H. Suzuki, C. Burrett, T. Htike, Z. Thein, T. Tsubamoto, N. Egi, and M. Maung. 2014. The oldest anthropoid primates in SE Asia: Evidence from LA-ICP-MS U-Pb zircon age in the Late Middle Eocene Pondaung Formation, Myanmar. Gondwana Research 26:122–131. doi:10.1016/j.gr.2013.04.007